

See discussions, stats, and author profiles for this publication at: <https://www.researchgate.net/publication/236327115>

An Observational Perspective on the Atmospheric Impacts of Alkyl and Multifunctional Nitrates on Ozone and Secondary Organic Aerosol

ARTICLE *in* CHEMICAL REVIEWS · APRIL 2013

Impact Factor: 46.57 · DOI: 10.1021/cr300520x · Source: PubMed

CITATIONS

23

READS

93

3 AUTHORS, INCLUDING:



A. E. Perring

National Oceanic and Atmospheric Administ...

96 PUBLICATIONS 1,665 CITATIONS

[SEE PROFILE](#)



Ronald C. Cohen

394 PUBLICATIONS 8,684 CITATIONS

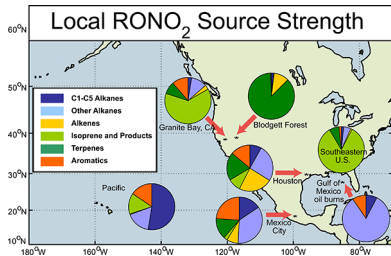
[SEE PROFILE](#)

An Observational Perspective on the Atmospheric Impacts of Alkyl and Multifunctional Nitrates on Ozone and Secondary Organic Aerosol

A. E. Perring,^{†,§,||} S. E. Pusede,[†] and R. C. Cohen*,^{†,‡}

[†]Department of Chemistry, and [‡]Department of Earth and Planetary Sciences, University of California Berkeley, Berkeley, California 94720, United States

Supporting Information



CONTENTS

1. Introduction
 2. Sources and Sinks of RONO₂
 - 2.1. OH-Initiated RONO₂ Formation
 - 2.2. NO_x-Initiated RONO₂ Formation
 - 2.3. The Fate of RONO₂ Molecules
 3. Observations of Individual RONO₂ and \sum ANs
 - 3.1. Measurements of Individual RONO₂
 - 3.2. Measurements of \sum ANs
 4. RONO₂ and Local O_x Production
 - 4.1. The Mechanistic Relationship between O_x and \sum ANs
 - 4.2. Observed Relationships between O_x and \sum ANs
 - 4.3. Implications for Ozone Control Strategies and Models
 5. Export of RONO₂ and NO_x on Regional to Global Scales
 6. RONO₂ and SOA Formation
 7. Conclusions and Recommendations for Future Work
- Associated Content
- Supporting Information
- Author Information
- Corresponding Author
- Present Addresses
- Notes
- Biographies
- Acknowledgments
- Abbreviations
- References

1. INTRODUCTION

Reactive nitrogen oxides are fundamental to the chemistry of atmospheric oxidation and affect air quality, climate, and ecosystem nutrient cycling. Nitrogen oxides interact nonlinearly with HO_x radicals (HO_x ≡ OH + HO₂ + RO₂) to both catalyze ozone (O₃) formation and terminate the HO_x catalytic chain and suppress O₃ (Figure 1). This interplay doubly affects the formation of secondary organic aerosol (SOA) by controlling the rate of organic oxidation and also the balance between organic peroxide and organic nitrate production, products of VOC oxidation with distinctly different propensities for incorporation into aerosol. Quantifying this chemistry is of consequence as O₃ is a toxic air pollutant, a greenhouse gas, an oxidant itself, and the major source of the hydroxyl radical (OH), the primary atmospheric oxidant. Likewise, the total aerosol burden, a large fraction of which is SOA, is known to cause adverse health effects¹ and to influence climate both directly and indirectly by altering the Earth's radiation balance.^{2,3}

Nitrogen oxides enter the atmosphere primarily as NO. They are oxidized first to NO₂ and then to organic nitrates, including peroxy nitrates (RO₂NO₂) and more strongly bound mono- and multifunctional alkyl nitrates (RONO₂), and nitric acid (HNO₃). Historically, the chemistry of RONO₂ has been among the most difficult to establish as the analytical tools for detection (typically aimed at individual nitrate species) were not ideal given the number of likely nitrates in the global atmosphere and the complexity of the chemistry governing their production, transformation, and removal. Fifteen years ago, Cohen and colleagues took a new approach to this question and developed a method for the quantification of the sum of all molecules of the chemical form R-ONO₂, referred to hereafter as \sum ANs.⁴ These \sum ANs measurements have since led both to a new appreciation for the wide importance of RONO₂ and to more nuanced thinking about the role these molecules play in the chemistry of the atmosphere. More recently, several mass spectrometry-based techniques have emerged that are capable of measuring a wide suite of multifunctional nitrates of high atmospheric relevance.^{5–7} These measurements allow detailed identification and quantification of VOC oxidation products, including many multifunctional nitrate species, through several steps of oxidation.

Received: December 21, 2012

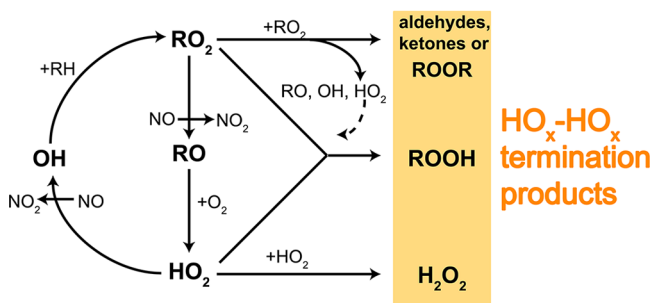
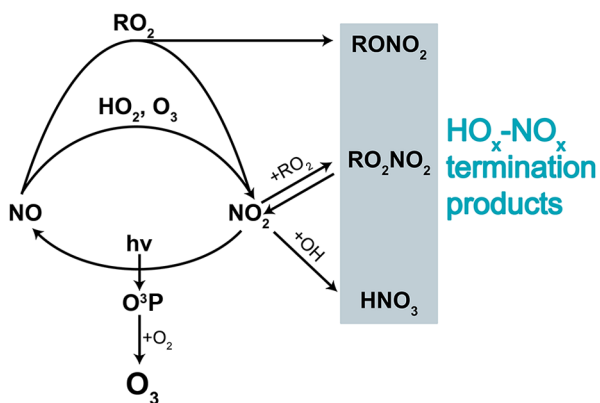
a The HO_x cycle**b The NO_x cycle**

Figure 1. (a) The HO_x radical cycle resulting in the production of O₃ and regeneration of OH in the presence of NO_x and the termination products formed from HO_x-HO_x self-reactions at low NO_x. (b) The NO_x radical cycle (coupled to the HO_x cycle) and the termination products formed from interactions between HO_x and NO_x at mid- and high-NO_x levels.

Here, we present a review of the atmospheric chemistry of alkyl and multifunctional nitrates with a focus on synthesizing recent laboratory and ambient observations. We build on the comprehensive reviews by Roberts⁸ and Shepson⁹ and

summarize recent progress in understanding production and loss mechanisms of RONO₂, methods for measuring ambient RONO₂, and in determining the influence of RONO₂ on tropospheric O₃ and SOA on local to global scales. Specifically, we outline processes leading to the formation and removal of RONO₂ (section 2). We then describe Σ AN measurements along with those of specific individual gas-phase RONO₂ (section 3). We examine relationships of dominant RONO₂ organic precursor molecules in urban, suburban, and rural locations with gas-phase Σ AN observations and discuss the constraints these observations place on aspects of the chemistry that are poorly or not at all characterized in the laboratory (section 4). We highlight areas of uncertainty in RONO₂ chemistry that have the greatest ramifications for local, regional, and global tropospheric chemistry, particularly the recycling (release) of NO_x (NO_x \equiv NO + NO₂) downwind of RONO₂ formation (section 5). We describe ambient observations of aerosol-phase RONO₂ and relationships between RONO₂ and SOA formation (section 6). To conclude, we present suggestions for future research (section 7).

2. SOURCES AND SINKS OF RONO₂

There are two main pathways for the chemical production of RONO₂: (1) hydroxyl radical (OH)-initiated oxidation of hydrocarbons in the presence of NO_x (daytime) and (2) nitrate radical (NO₃)-initiated oxidation of alkenes (nighttime). Methyl nitrate (CH₃ONO₂), ethyl nitrate (C₂H₅ONO₂), and possibly propyl nitrate (C₃H₇ONO₂) are directly emitted from oceans and up to tens of ppt of these species have been measured in remote marine locations.^{10–13} Otherwise emissions are not considered an important source of RONO₂. RONO₂ have vapor pressures that span many orders of magnitude and are found in the atmosphere in both the gas and the aerosol phases. Following the initial production, RONO₂ can undergo chemical transformations that leave the nitrate group intact but change the level of functionality and vapor pressure. They are removed by chemical reactions resulting in the loss of the nitrate functional group, by deposition to the Earth's surface, and, to a limited extent, by

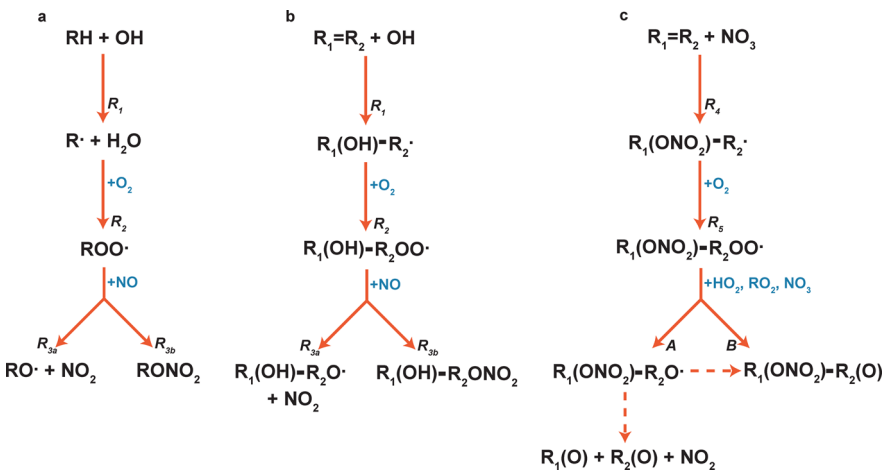


Figure 2. (a) Schematic of reactions R1–R3 for an alkane initiated by OH resulting in the production of either a stable, monofunctional alkyl nitrate or an alkoxy radical and NO₂. (b) Schematic of reactions R1–R3 for an alkene initiated by OH addition to the double bond and resulting in the production of a hydroxyl alkyl nitrate or a hydroxyl-alkoxy radical and NO₂. (c) Schematic of reactions R4 and R5 for NO₃ oxidation of an alkene. In the notation, the functional group is in parentheses; for example, R₁(O) and R₁(OH) represent carbonyl and hydroxyl groups, respectively.

Table 1. Values of k_{OH} and α Used for Calculations of OH Reactivity, $P(\text{O}_3)$, and $P(\sum \text{ANs})^a$

| | k_{OH} | α | | k_{OH} | α |
|-----------------------|------------------------|--------------|------------------------|------------------------|--------------|
| Alkanes | | | | | |
| methane | 6.34×10^{-15} | 0.0005 (1) | 2,2-dimethylpentane | 3.40×10^{-12} | 0.1 |
| ethane | 2.48×10^{-13} | 0.019 (2) | 2,2,4-trimethylpentane | 3.34×10^{-12} | 0.14 |
| propane | 1.09×10^{-12} | 0.036 (3) | methylcyclopentane | 5.60×10^{-12} | 0.14 |
| <i>n</i> -butane | 2.36×10^{-12} | 0.077 (3) | hexane | 5.20×10^{-12} | 0.141 (4) |
| <i>n</i> -pentane | 3.80×10^{-11} | 0.105 (4) | cyclohexane | 6.97×10^{-12} | 0.16 (5,6,9) |
| <i>i</i> -butane | 2.12×10^{-12} | 0.096 (5,6) | methylcyclohexane | 9.64×10^{-12} | 0.17 |
| <i>i</i> -pentane | 3.60×10^{-12} | 0.07 (5,6,7) | heptane | 6.76×10^{-12} | 0.178 (4) |
| 2,2-dimethylbutane | 2.23×10^{-12} | 0.152 | octane | 8.11×10^{-12} | 0.226 (4) |
| cyclopentane | 4.97×10^{-12} | 0.045 (5,8) | nonane | 9.70×10^{-12} | 0.393 |
| 2-methylpentane | 5.20×10^{-12} | 0.097 (7) | decane | 1.10×10^{-11} | 0.417 |
| 3-methylpentane | 5.20×10^{-12} | 0.109 | | | |
| Alkenes | | | | | |
| ethene | 8.52×10^{-12} | 0.0086 (10) | t2-butene | 6.40×10^{-11} | 0.034 |
| propene | 2.63×10^{-11} | 0.015 (10) | c2-butene | 5.64×10^{-11} | 0.034 (10) |
| 1-butene | 3.14×10^{-11} | 0.025 (10) | 1-pentene | 3.14×10^{-11} | 0.059 |
| methylpropene | 5.14×10^{-11} | 0.012 | t2-pentene | 6.70×10^{-11} | 0.064 |
| 2-methyl 1-butene | 6.10×10^{-11} | 0.02 | c2-pentene | 6.50×10^{-11} | 0.064 |
| 3-methyl 1-butene | 3.18×10^{-11} | 0.059 | butadiene | 6.66×10^{-11} | 0.07 (11) |
| 2-methyl 2-butene | 8.69×10^{-11} | 0.034 | 1-hexene | 3.70×10^{-11} | 0.055 (10) |
| Isoprene and Products | | | | | |
| isoprene | 1.00×10^{-10} | 0.07 (12,13) | MVK | 2.00×10^{-11} | 0.11 (14) |
| MACR | 2.90×10^{-11} | 0.15 (14) | | | |
| Terpenes | | | | | |
| α -pinene | 5.23×10^{-11} | 0.18 (15) | limonene | 1.64×10^{-10} | 0.23 |
| β -pinene | 7.43×10^{-11} | 0.24 | 3-carene | 8.80×10^{-11} | 0.23 |
| Aromatics | | | | | |
| benzene | 1.22×10^{-12} | 0.034 (16) | <i>m</i> -xylene | 2.30×10^{-11} | 0.074 |
| Prbenzene | 5.80×10^{-12} | 0.093 | <i>p</i> -xylene | 1.43×10^{-11} | 0.097 |
| toluene | 5.96×10^{-12} | 0.029 (16) | ethylbenzene | 7.00×10^{-12} | 0.072 |
| 2Ethyltoluene | 1.19×10^{-11} | 0.106 | 1,3,5-trimethylbenzene | 5.76×10^{-11} | 0.031 (16) |
| 3Ethyltoluene | 1.86×10^{-11} | 0.094 | 1,2,4-trimethylbenzene | 3.25×10^{-11} | 0.105 |
| 4Ethyltoluene | 1.18×10^{-11} | 0.137 | 1,2,3-trimethylbenzene | 3.25×10^{-11} | 0.119 |
| <i>o</i> -xylene | 1.36×10^{-11} | 0.081 | isopropylbenzene | 6.30×10^{-12} | 0.11 |
| Other | | | | | |
| CO | 2.39×10^{-13} | 0 | acetaldehyde | 1.58×10^{-11} | 0 |
| H_2CO | 8.37×10^{-12} | 0 | | | |

^aAll OH reaction coefficients are from Atkinson and Arey.¹⁴⁰ References for RONO_2 formation branching ratios are as follows: (1) Flocke et al.;⁹⁶ (2) Ranschaert et al.;²³⁵ (3) Atkinson et al.;²⁰ (4) Arey et al.;²¹ (5) Lightfoot et al.;²³⁶ (6) Le Bras et al.;²³⁷ (7) Atkinson et al.;²³⁸ (8) Takagi et al.;²³⁹ (9) Aschmann et al.;²⁴⁰ (10) O'Brien et al.;²² (11) Tuazon et al.;³⁷ (12) Patchen et al.;⁴⁰ (13) Lockwood et al.;⁴¹ (14) Paulot et al.;⁷ (15) Noiziere et al.;¹⁶ and (16) Elrod et al.³⁵ Branching ratios for compounds for which no experimental data exist (marked in bold) are as found in the Leeds Master Chemical Mechanism where they have been estimated on the basis of structure-reactivity relationships.

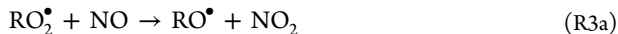
photolysis. In this section, we give a brief account of each of these mechanisms.

2.1. OH-Initiated RONO_2 Formation

OH attack on a saturated hydrocarbon (R1) proceeds by H-abstraction and is almost immediately followed by addition of O_2 to generate an RO_2 radical (R2).



In the presence of NO_x , RO_2 reacts with NO with two product channels (R3a and R3b).



R3a is the dominant channel, and it propagates the NO_x and HO_x catalytic cycles (Figure 1) with products that are NO_2 and an alkoxy radical. The minor channel, R3b, is chain terminating and forms a stable monofunctional organic nitrate (Figure 2a). This general pattern has minor variations that depend on the identity of R. In the case of an alkyl-substituted aromatic ring, for example, H-abstraction likely occurs at the alkyl group, and R3b yields a benzyl alkyl nitrate. For a molecule with a carbon backbone of 4 or greater, the alkoxy radical produced by R3a may undergo intramolecular H-abstraction by the O terminus forming a hydroxy alkyl radical via a six-membered ring intermediate. The product R^\bullet then reacts by R2 to reform an RO_2 radical and has a second opportunity to produce an RONO_2 via reaction R3b. This pathway converts alkanes into δ -hydroxynitrates, molecules with subsequent chemistry that is distinct from that of monofunctional RONO_2 .

Figure 2b shows the oxidation of an unsaturated organic molecule; the notable difference is that OH oxidation proceeds by addition rather than by H-abstraction and results in the production of β -hydroxynitrates. This pathway applies, for example, to the formation of hydroxy nitrates from the oxidation of isoprene, discussed below, and also to α -pinene-derived hydroxyl nitrates.^{14–16} Alternatively, the hydroxy alkoxy radical can isomerize through a 1,5 H-shift (as described above) producing a dihydroxy alkyl radical that can react by R2 and R3b to yield a dihydroxy nitrate.¹⁷ Compounds with multiple carbon–carbon double bonds subsequently oxidize following this same pathway also potentially forming multifunctional dinitrates.^{7,18}

RO_2 also reacts with NO_2 to form peroxy nitrates (RO_2NO_2) (not shown) on time scales comparable to RONO_2 formation. RO_2NO_2 are thermally labile and rapidly dissociate at ambient temperatures. Generally, RO_2NO_2 only affect RONO_2 by modifying the available NO_x . Readers interested in RO_2NO_2 chemistry are directed to reviews by Roberts et al.^{8,19}

The R3b branching ratio (α), the ratio $k_{3b}/(k_{3a} + k_{3b})$, varies between 0.1–35%.^{20,21} Although the α 's for many atmospherically important molecules have yet to be quantified in the laboratory, trends in alkanes and monoalkenes are well understood. Table 1 shows values of α measured in the laboratory for a variety of molecules. Many product studies report nitrate yields for specific RO_2 radical isomers rather than total nitrate yields. In these cases, overall nitrate yields have been calculated using reported nitrate yields for individual RO_2 radicals along with estimations of the relative production of RO_2 isomers taken from the Leeds Master Chemical Mechanism. Alkanes typically have α values that are about a factor of 2 higher than alkenes with an equivalent number of carbon atoms; the presence of a hydroxyl group β to the peroxide group in the peroxy radical weakens the O–O bond in the ROONO^* intermediate and makes dissociation to NO_2 and an alkoxy radical more likely.²² Larger molecules in both sequences have higher α , likely because an increased number of vibrational degrees of freedom enhances the stabilization of the reaction intermediate.²³ These trends for alkanes and 1-alkenes as well as a few other compounds are shown in Figure 3a.

The pressure and temperature dependences of RONO_2 formation are typical of association reactions; α increases with increasing pressure and decreases with increasing temperature.^{23–30} The α of ethyl nitrate formation, for example, decreases by about a factor of 2 from the low temperatures characteristic of the upper troposphere (215 K) to the Earth's surface (298 K).²⁴ The temperature dependence for pentyl nitrate formation from *n*-pentane is shown in Figure 3b. The dependence on the size of the hydrocarbon backbone and pressure and temperature is interpreted as evidence for a mechanism that proceeds through the formation of a vibrationally excited ROONO^* adduct followed by a three-membered ring transition state to produce RONO_2^* that is then collisionally stabilized.^{20,31,32} This mechanism may not hold however for aromatic compounds, species for which the nitrate formation mechanism has been little studied. Older studies (e.g., those from the Atkinson group^{33,34}) found low (<5%) nitrate yields from OH-initiated oxidation of aromatic compounds, but carbon and nitrogen closure were incomplete, possibly due to the formation of unidentified ring-opening products. More recently, Elrod measured α for a variety of aromatics and found no pressure dependence and that the yield decreased with increasing methyl substitution to the ring.³⁵

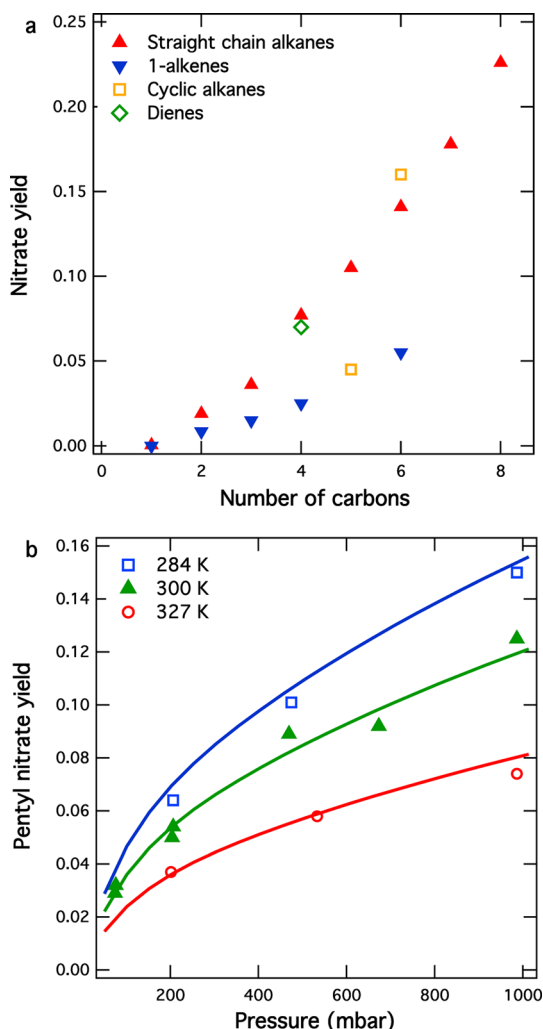


Figure 3. (a) Nitrate formation yield as a function of the length of the carbon backbone for alkanes, 1-alkenes, butadiene, cyclopentane, and cyclohexane. See Table 1 for yield references. (b) Pressure and temperature dependence of the nitrate yield from OH-initiated oxidation of *n*-pentane reported by Atkinson et al.²³ Symbols represent experimental results; lines represent the general falloff equation for simple addition reactions as parametrized in this Review.

Isoprene is a C₅ dialkene emitted to the atmosphere from the biosphere (mostly from deciduous trees) in larger quantities than any other single organic molecule except methane.³⁶ As a result, isoprene nitrates (INs) are expected to be present in relatively high concentrations and to play an important role in the chemistry of the atmosphere. Laboratory studies report OH-initiated nitrate formation yields of isoprene varying from 4–15%.^{7,37–40} The more recent experiments suggest that a range of 7–12% is most likely, which is consistent with structurally similar alkenes.^{7,40,41} Some of the variability in these laboratory results may result from losses of INs during sampling⁴¹ or from the short lifetime of the INs themselves to oxidation such that experiments with longer residence times are subject to larger losses and lower apparent yields.⁷ Each of the eight IN isomers has a different yield and chemical lifetime (due to the location and substitution of the unoxidized double bond), which means that the abundance and atmospheric impact of INs as a class are determined by the differential production and variable fates of each of the products.⁴² To date, there remains uncertainty about the yield of each first-

generation IN (see Table 1 in Lockwood et al.⁴¹). Paulot et al.⁷ report that the oxidation products of δ -hydroxy nitrates include propanal nitrate (PROPN) and ethanal nitrate (ETHLN). Both of these species as well as methyl vinyl ketone nitrate (MVKN) and methacrolein nitrate (MACRN), derived from the first generation isoprene oxidation products methacrolein and methyl vinyl ketone, have recently been measured in the atmosphere.⁵

2.2. NO₃-Initiated RONO₂ Formation

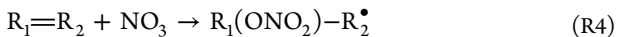
Whereas daytime formation of RONO₂ is dominated by the OH-initiated pathway discussed above, RONO₂ are produced at night from reactions of NO₃ with alkenes and phenols (Figure 2c) with α in the range of 20–80%.^{43–52} As a result of these high yields, the NO₃ source could be responsible for as much as 50% of RONO₂ on a regional scale despite representing a small fraction of the total oxidation of organics as compared to OH.⁵³ A compilation of results for alkene and phenolic species reacting with NO₃ is presented in Table 2.

Table 2. Reaction Rate Constants and Nitrate Yields for Reactions of NO₃ with Select Alkenes^a

| compound | k_{NO_3} | nitrate yield |
|-----------------------|----------------------------|------------------|
| propene | 9.5×10^{-15} (1) | 0.58 (3) |
| isobutene | 3.32×10^{-11} (1) | 0.25 (3) |
| 1-butene | 1.35×10^{-14} (1) | 0.60 (3) |
| t2-butene | 3.9×10^{-13} (1) | 0.57 (3,4) |
| 1,3-butadiene | 1.0×10^{-13} (1) | 0.6 (3) |
| isoprene | 6.78×10^{-13} (1) | 0.7 (3,5,6) |
| 2,3-dimethyl 2-butene | 5.72×10^{-13} (1) | 0.05 (4) |
| cyclopentene | 5.3×10^{-13} (1) | 0.3 (7) |
| cyclohexene | 5.9×10^{-13} (1) | 0.52 (7) |
| methylcyclohexene | 1.7×10^{-11} (1) | 0.24 (7) |
| α -pinene | 6.16×10^{-12} (1) | 0.15 (8,9,10,11) |
| β -pinene | 2.51×10^{-12} (1) | 0.4 (12) |
| limonene | 1.22×10^{-11} (1) | 0.67 (10) |
| phenol | 3.92×10^{-12} (2) | 0.251 (2) |
| <i>o</i> -cresol | 1.37×10^{-11} (2) | 0.128 (2) |
| <i>m</i> -cresol | 9.74×10^{-11} (2) | 0.364 (2) |
| <i>p</i> -cresol | 10.7×10^{-12} (2) | 0.74 (2) |

^aRate constant data for most species are from (1) Atkinson and Arey⁴⁰ except for phenolic species, which are from (2) Atkinson et al.²⁴¹ References for nitrate yields are as follows: (3) Barnes et al.,⁴⁸ (4) Hjorth et al.,⁴⁷ (5) Perring et al.,⁴⁴ (6) Rollins et al.,⁵¹ (7) Wangberg et al.,⁴⁹ (8) Berndt et al.,⁵⁰ (9) Noziere et al.,¹⁶ (10) Splitter et al.,⁴⁵ (11) Wangberg et al.,⁵⁵ and (12) Fry et al.⁴³

In the first step, NO₃ adds to a double bond R4, and, as in R2, the alkyl radical rapidly combines with O₂ to form a peroxy radical R5.



This peroxy radical then reacts with HO₂, RO₂, or NO₃ to generate a stable aldehyde- or alcohol-nitrate product. Reaction with NO (R3a and R3b) is unimportant in the atmosphere as NO₃ cannot be present in appreciable quantities in the presence of NO (NO and NO₃ rapidly combine to yield two NO₂). Nitrooxy-peroxynitrates (R₁(ONO₂)-R₂O₂NO₂) from the reaction of nitrooxy-peroxy radicals with NO₂ have also been observed as short-lived products in the laboratory,^{47–49,54,55} however, they are highly thermally unstable,

have not been reported in ambient observations, and are more likely to affect interpretation of laboratory experiments than to be directly important to the chemistry of the atmosphere. It is possible for NO₃ to oxidize alkanes via H-atom abstraction, but this process is too slow to be atmospherically relevant.

2.3. The Fate of RONO₂ Molecules

Once formed, a gas-phase RONO₂ molecule can be transported by winds, undergo chemistry, deposit to the Earth's surface, or be incorporated into aerosol (Figure 4). For any given starting nitrate, its particular structure will determine the rates of further oxidation (k_{R1}) and of deposition or incorporation into aerosol (k_{D1}). More highly functionalized nitrates (either first generation multifunctional nitrates or nitrates that become multifunctional over multiple oxidation steps) are expected to have higher k_{D} values, while nitrates that retain a double bond or that have hydrogen atoms available for abstraction will have higher k_{R} values. For example, in the case of first generation INs, reactions with O₃ and OH are fast, and lifetimes for all eight isomers against daytime oxidation are thought to be less than a few hours.⁴¹ Similarly, continued oxidation will cause later generation products to have different k_{Rx} and k_{Dx} values than the starting material. The products of OH, O₃, and NO₃-initiated oxidation of RONO₂ molecules are not generally well-known; however, it is reasonable to assume that the chemistry consists of two pathways. In one pathway (labeled β in Figure 4), oxidation results in a stable multifunctional nitrate, R₁ONO₂, where the original carbon backbone R is modified and the new R₁ backbone has acquired additional functionalization (e.g., carbonyl, alcohol, or nitrate group). Alternatively, oxidation can result in the release of NO₂ and the loss of the nitrate group (labeled (1 – β) in Figure 4). As we discuss in detail below, the extent to which the chemistry proceeds along one or the other of these two paths remains one of the largest uncertainties in our understanding of the atmospheric chemistry of RONO₂, O₃, and SOA.

Aschmann et al.⁵⁶ observed in laboratory experiments that the short- and branched-chain alkyl nitrates 2-propyl nitrate, 3-methyl-2-butyl nitrate, and 3-methyl-2-pentyl nitrate released NO₂ upon OH-initiated oxidation. In contrast, the same group found that reactions between OH and longer, linear alkyl nitrates (e.g., 2- and 3-hexyl nitrate) were likely to result in retention of the nitrate functionality.⁵⁷ This behavior is attributed to differences in intermediate alkoxy radical reaction pathways, whereby isomerization and reaction with O₂ lead to multifunctional nitrates, while alkoxy radical decomposition leads to the formation of carbonyls and the release of NO₂. Thus, the structure of the starting nitrate determined the balance between maintaining the nitrate functional group (β) and the release of NO₂ (1 – β). These experiments indicate that higher values of β (greater nitrate retention) are expected if the nitrate group is well separated from the most reactive hydrogen atoms or remaining double bonds.

Monofunctional RONO₂, with Henry's law constants of 2.64 M/atm for methyl nitrate and a decreasing trend for larger nitrates, are barely water-soluble and are not removed by deposition.⁵⁸ Multifunctional nitrates and in particular hydroxy nitrates are of special interest as they have been measured to be highly water-soluble with Henry's law constants in the range of 1×10^4 M/atm (1-nitro-2-butanol) to 6.5×10^4 (nitrooxyethanol)^{59–61} as compared to 2.1×10^5 for HNO₃.⁶² The Henry's law solubility likely sets the deposition rates of these multifunctional RONO₂ as well as the rate of aerosol uptake in

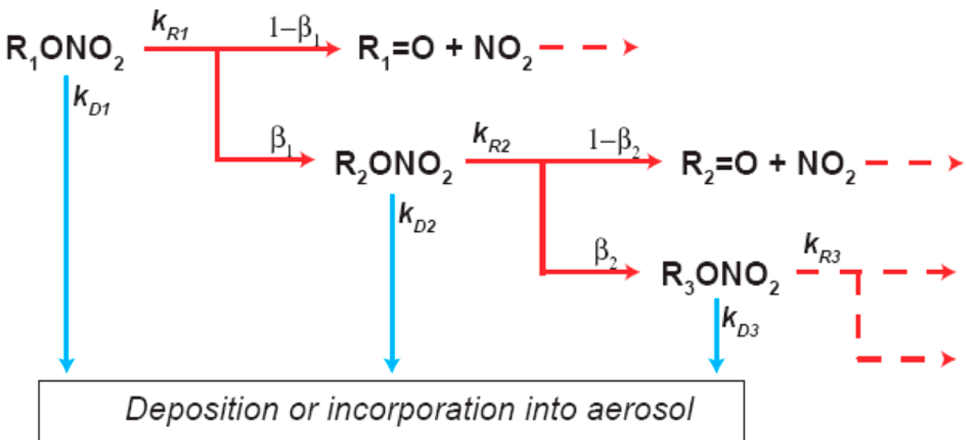


Figure 4. Schematic of the possible fates of a generic RONO₂ molecule. The k_D 's represent rates of depositional loss and will depend on the specific structure of the molecule, k_R 's are oxidation rates by either OH or O₃, and β 's represent branching between nitrate retention and release of NO_x. The numbered R subscripts indicate that the exact identity and functionalization of the R group may change in subsequent generations.

wetter environments. Surrogates for their sum have been observed to contribute significantly to wet and dry nitrogen deposition in forested environments,^{63–65} and direct flux measurements of Σ ANs support this point.⁶⁵

Multifunctional RONO₂ have also been shown to have lower vapor pressures than their monofunctional analogs. Vapor pressures for monofunctional RONO₂ molecules even as large as \sim C₁₂ are too high to favor partitioning to aerosol.^{15,59,66} For these species, chemical reaction is the most important process determining their fate, although further oxidation is likely to yield molecules that do partition into aerosol significantly. Multifunctional β -hydroxy nitrates and dinitrates derived from large 1-alkenes (C₈–C₁₇) and nonterminal alkenes (C₁₄–C₁₇) have been seen to completely partition to the aerosol phase for $>$ C₁₀.⁶⁷ The role of RONO₂ in the formation of SOA is discussed in more detail in section 5.

RONO₂ molecules are photolabile in the near UV ($\lambda < 340$ nm) producing RO[•] and NO₂ with near unity quantum efficiencies. The rates of photolysis have been measured for a variety of C₁–C₅ alkyl and cycloalkyl nitrates^{68–75} as well as for a number of difunctional organic nitrates.^{70,76} These rates are rapid enough for small nitrates (C₁–C₄) that photolysis is competitive with oxidation by OH ($\tau_{\text{photolysis}} \sim 3$ days for *t*-butyl nitrate to ~ 10 days for methyl nitrate in summer at the surface with a zenith angle of 0°); even faster rates have been observed for compounds with a carbonyl group α to the –ONO₂ group ($\tau_{\text{photolysis}} \sim 6$ h for 3-nitrooxy-2-butanone to ~ 1 day for propanediol nitrate in summer at the surface). Otherwise, RONO₂ photodissociation rates are slow as compared to OH reaction, and, for larger nitrooxy alkanes and alkenes, photolysis is minor or negligible.

3. OBSERVATIONS OF INDIVIDUAL RONO₂ AND Σ ANs

Ambient observations of gas-phase RONO₂ include measurements of individual RONO₂ species,^{13,77–81} measurements of Σ ANs,^{82–86} and inferences of total RONO₂ by subtracting the sum (or most) of the non-RONO₂ components from the total measured NO_y (NO_y ≡ NO + NO₂ + RO₂NO₂ + RONO₂ + HNO₃ + HONO + NO₃ + 2N₂O₅ + ...).^{8,87–89} The first indication that RONO₂ was an important class of NO_y was the observation of a 5–40% gap in the NO_y budget.^{90–92} This gap exhibited seasonal and diurnal dependencies such that it was

largest during the daytime and in the summer. Meanwhile, calculations suggested that a wide array of alkyl and multifunctional RONO₂ should be present in the atmosphere.^{93,94} However, the first observations of specific RONO₂ in the troposphere (Atlas⁸¹) provided little experimental evidence for a large contribution by monofunctional alkyl nitrates to the total NO_y and no information on multifunctional compounds. This was in part a result of instrumental limitations that confined detection to short-chain monofunctional nitrates rather than to the hydroxy and dinitrates predicted to be present in large abundances. RONO₂ are arguably the most difficult class of NO_y to measure in situ due to both the wide variety of RONO₂ molecules and their often highly functionalized structures; as such, these analytical challenges have greatly shaped the observational and intellectual approaches to the study of RONO₂.

3.1. Measurements of Individual RONO₂

Atlas⁸¹ reported tens of ppt of C₃–C₅ alkyl nitrates in the troposphere and showed that they were positively correlated with radon, indicative of continental and most likely urban sources and suggesting subsequent transport to the remote marine troposphere where the observations were obtained. Even as larger nitrates were included in the observations, most studies continued to conclude that the sum of all individually measured monofunctional RONO₂ was a very small fraction of NO_y.^{80,95–97} The majority of these studies used gas chromatography with electron capture detection (GC–ECD). Some injected air samples directly onto the column,⁹² while others collected the nitrates on filters for analysis following extraction with organic solvents or thermal desorption of the collected compounds.^{77,80,81,95} Luxenhofer and colleagues^{80,97–99} used a combination of GC–ECD and GC with mass spectrometric identification (GC–MS). These studies along with parallel modeling studies confirmed RONO₂ derived from alkanes were transported from polluted regions to remote marine environments and, as such, were especially useful as tracers of anthropogenic influence on the remote atmosphere.^{100–103} Ratios of nitrates to their parent hydrocarbons have also been used as photochemical clocks measuring time from an urban source to remote regions.¹⁰⁴

Measurements of multifunctional nitrates are more difficult as the lower vapor pressures and stronger surface interactions of these molecules make sampling and chromatographic

separation more challenging. Despite these operational challenges, for every VOC precursor for which a technique exists to measure the related product nitrate, the corresponding RONO_2 has been observed in the atmosphere when the precursor is abundant. O'Brien et al.⁷⁷ were the first to report ambient measurements of multifunctional nitrates. They detected 17 RONO_2 including 4 $\text{C}_2\text{--C}_4$ hydroxy nitrates and 1 dinitrate in northern Ontario and later observed a larger suite of multifunctional nitrates in the suburbs of Vancouver. Papers by Kastler and colleagues identified 30 dinitrates and a number of hydroxy nitrates ($\text{C}_2\text{--C}_7$) over central Europe using preseparation by high-pressure liquid chromatography (HPLC) followed by GC-ECD and GC-MS.^{105–107} Fischer and colleagues⁷⁹ reported observations of 66 RONO_2 aboard the German RV Polarstern, including 23 dinitrates and 7 hydroxy nitrates. Kastler et al.¹⁰⁸ first quantified many of these speciated nitrates, identifying 43 mononitrates ($\text{C}_6\text{--C}_{13}$), 24 dinitrates ($\text{C}_3\text{--C}_6$), and 19 hydroxy nitrates ($\text{C}_2\text{--C}_6$) and finding the summer noontime abundances of the sum of the calibrated subset to range from 2.9–11.0 ppt (15 mononitrates), 2.3–10.5 ppt (21 dinitrates), and 7.3–28 ppt (7 hydroxy nitrates).

The regional and global importance of isoprene nitrates (INs) makes their observations of particular importance with several groups having developed measurement techniques to observe these nitrates in ambient samples. Observations of INs were first reported by Werner et al.,¹⁰⁹ but concentrations were not quantified. Grossenbacher et al.¹¹⁰ and Thornberry et al.¹¹¹ provided the first quantitative measurements of INs above a northern Michigan forest using preconcentration on a filter followed by thermal desorption and then GC-ECD. At this site, concentrations of INs reached ~35 ppt and were typically less than 2% of NO_y . Grossenbacher et al.¹¹² later reported IN concentrations at a forested site in Tennessee that were an order of magnitude higher and ~5% of NO_y using the same methods. Correlations between INs and other isoprene oxidation products were similar at both sites, and so the difference in abundance was attributed to the local oxidant levels. INs were measured at the Michigan site again in 2000, and Giacopelli et al.⁴² compared the observed concentrations to calculations using a detailed chemical model. The measurements were a factor of 2 lower than computed, and the model predicted significant concentrations of three isomers while only two were detected in ambient samples. Because the different isomeric structures are expected to have different oxidative lifetimes, both the lower than expected concentrations and the absence of one of the dominant isomers were attributed to chemical loss. The authors suggested that first generation INs were oxidized and converted into more highly functionalized nitrates.

In chamber studies, INs produced by OH-initiated oxidation have been observed by atmospheric pressure ionization mass spectrometry (API-MS)¹¹³ and proton transfer reaction mass spectrometry (PTR-MS),^{6,44} but quantitative ambient measurements using these techniques are not yet routine. In a recent analytical advance, Beaver et al.⁵ reported observations of INs using chemical ionization mass spectrometry (CIMS) made during the BEARPEX 2009 field experiment in the Sierra Nevada Mountains in California. That study found that the sum of the 8 first generation isoprene hydroxy nitrates was typically ~150 ppt and, on a few days, greater than 400 ppt. They also quantified 4 second generation isoprene nitrates: PROPNN (~30 ppt), ETHLN (~20 ppt), and the sum of MVKN +

MACRN, which are isobaric (~40 ppt), as well as ~25 ppt 2-methyl-3-buten-2-ol nitrates (MBON), which are derived from MBO, an important local biogenic organic compound.¹¹⁴

3.2. Measurements of Σ ANs

Day et al.⁴ describe an analytical technique to measure Σ ANs (the sum of all compounds of the form RONO_2) that both effectively closes the NO_y budget and is capable of tracking RONO_2 through multiple steps of oxidation. This approach works by exploiting the thermal dissociation (TD) of three reservoirs of reactive nitrogen at characteristic temperatures to produce NO_2 (which is then measured) and a companion radical. In the UC Berkeley system, NO_2 is detected by laser-induced-fluorescence (LIF).¹¹⁵ The Berkeley TD-LIF operates with sampling inlets held at four temperatures: unheated, ~200 °C, ~350 °C, and ~550 °C. The unheated temperature channel measures NO_2 , while the 200 °C channel detects ambient NO_2 plus the NO_2 generated from the dissociation of acyl peroxy nitrates, pernitric acid, and N_2O_5 (Σ PNs). The ~350 °C channel detects ambient NO_2 , Σ PNs, and NO_2 from Σ ANs. The inlet at ~550 °C measures all prior categories of NO_2 and the NO_2 generated from dissociation of HNO_3 (Figure 5). This

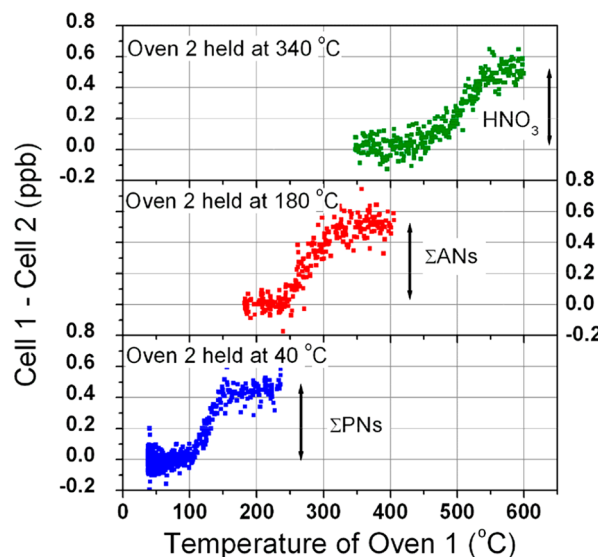


Figure 5. From Murphy et al.¹¹⁷ TD-LIF mixing ratio versus oven temperature showing the difference in NO_2 detected between two detection cells (numbered 1 and 2) as the temperature of oven 1 is cooled from above that of oven 2 to the same temperature. The center panel shows that when ovens 1 and 2 are set to 340 and 180 °C, respectively, the difference in NO_2 mixing ratio gives the total alkyl nitrates (Σ ANs). The two channels agree when the ovens are near the same temperature. Note the clear plateaus between classes of compounds; for example, when the oven is anywhere between 160 and 230 °C essentially all of the Σ PNs have dissociated while no Σ ANs have. Each data point represents a 3 s average during a daytime scan of the ambient atmosphere at Big Hill in California.

instrument is equipped with either two or four detection cells so that the NO_2 signals in channels at adjacent temperatures can be monitored simultaneously. The concentration of any given class of compounds is then inferred as the difference in NO_2 signal between the two channels. To calculate Σ ANs, for example, the signal in the 200 °C channel ($\text{NO}_2 + \Sigma$ PNs) is subtracted from that in the ~350 °C channel ($\text{NO}_2 + \Sigma$ PNs + Σ ANs). Analogously, Paul et al.¹¹⁶ describe a technique to measure NO_2 , Σ PNs, and Σ ANs by coupling TD to cavity

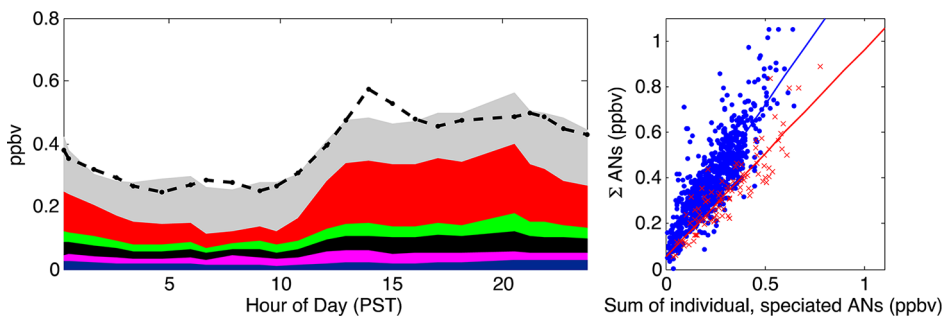


Figure 6. From Beaver et al.⁵ Comparison of CIMS spiculated RONO₂ measurements and UC-Berkley TD-LIF Σ ANs measurements. The left panel shows the diurnal profile of TD-LIF Σ ANs (dotted line) and spiculated RONO₂ by CIMS where red, green, black, magenta, and blue represent nitrates derived from isoprene, PROPNN, MCK+MACRN, MBO, and ethane, respectively. The gray fraction represents “unidentified” nitrates. The right panel shows the correlation between TD-LIF Σ ANs and the sum of all spiculated CIMS measurements. Red points show the correlation including the unidentified nitrate species (slope = 0.91), and blue points show the correlation without the unidentified nitrates (slope = 1.25).

ring-down spectroscopy (CRDS), where the NO₂ produced by TD is detected by CRDS rather than LIF; however, ambient measurements of TD-CRDS Σ ANs have not yet been reported.

Techniques built on thermal dissociation rely on the detection of NO₂ rather than the associated organic group so they are equally sensitive to all RONO₂, regardless of the structure of R, and are in this way able to observe nitrates through multiple oxidation reactions as long as the nitrate functionality is maintained. TD assumes that (1) all compounds of the form RONO₂ dissociate at roughly the same temperature and (2) no other forms of reactive nitrogen dissociate at that temperature. Experiments in the lab and the field support the first assumption without qualification.^{4,51,117} Concerning the second, recent work has shown nitryl chloride (ClNO₂) thermally dissociates at the same temperatures as RONO₂, and, as a result, ClNO₂ will positively interfere with field observations of Σ ANs.¹¹⁸ ClNO₂ is formed at night via a surface reaction involving N₂O₅ on chlorine containing aerosols.¹¹⁹ At sunrise, production stops with diminished N₂O₅ abundances, and ClNO₂ is lost through photolysis;¹²⁰ mid- and late-morning ClNO₂ concentrations have been observed at low ppt levels. ClNO₂ has been measured by CIMS at a number of sites, including inland locations, and in some cases has been seen to exceed 1 ppb in the dark;¹²¹ more typically ClNO₂ concentrations are in the ppt range.^{118,122,123} Daytime concentrations are negligible as compared to Σ ANs. A second possible interference to Σ ANs is from semivolatile nitropolycyclic aromatic hydrocarbons (nitro-PAHs). These compounds are either directly emitted by diesel engines or chemically formed during the oxidation of compounds such as naphthalene or methyl naphthalene.^{124–130} Experiments in the Cohen lab (Lee, personal communication) show that nitrobenzene thermally dissociates at temperatures greater than 550 °C, and we expect the C–N bond of related compounds to dissociate similarly.

Operationally, all channels in Berkeley TD-LIF systems are calibrated using NO₂ reference gas standards with stated certainties of $\pm 5\%$. The individual standards are compared on a regular basis (about every 6 months to ensure stability) and have been observed to both remain constant for up to 5 years and be accurate at atmospherically relevant mixing ratios to within 1%.¹³¹ The accuracy of Σ PN, Σ AN, and HNO₃ measurements includes terms for the completeness of thermal dissociation, experimentally shown to be near unity for these species,^{4,116} and for transmission through and for chemical

production and loss of NO₂ in the inlet. These additional uncertainties have been used to estimate the accuracy of the Berkeley TD-LIF as $\pm 15\%$, and these issues are quantified and described in detail in Day et al.⁴ and Wooldridge et al.¹³²

As mentioned in section 3.1, a key analytical consideration in the measurement of multifunctional RONO₂ is loss to surfaces during sampling and/or separation. Chromatographic techniques function on the principle that molecules can be separated on the basis of their different interactions with the surface of the column. As a result, it is generally expected that measurements employing separation prior to detection will be biased low, although a preconditioning step can reduce these losses. In the Berkeley TD-LIF, adsorptive losses to walls are minimized through an inlet design in which thermal dissociation occurs as close as possible to the entry point and NO₂ rather than multifunctional RONO₂ are delivered to the detection cell through the sampling lines. A reduction in pressure prior to or immediately following dissociation ensures against radical recombination. Experiments described in Day et al.⁴ and Farmer et al.¹³³ for HNO₃, a species thought to be even more prone to wall loss than multifunctional nitrates, show fast rise and fall time constants for the observed HNO₃ signal and indicate very small losses within the inlet.

The Berkeley LIF NO₂ measurement has been intercompared with other NO₂ measurements on multiple occasions, and agreement is generally better than 5%.¹³⁴ In addition to NO₂ intercomparisons, the other measured classes of NO_y have been intercompared where possible. A series of peroxy nitrate intercomparison exercises were performed in Boulder in the summer of 2005, and the Berkeley TD-LIF Σ PNs measurement generally agreed with the sum of spiculated peroxy nitrate measurements to within 10%.¹³² In a set of chamber experiments, the Berkeley TD-LIF was operated alongside a PTR-MS while sampling a synthesized isoprene nitrate standard of two δ -hydroxy nitrate isomers and while sampling from the chamber during an NO₃-initiated isoprene oxidation experiment involving a complex mixture of keto and hydroxy nitrate isomers. Under both conditions, the two measurements agreed to within 10%. A comparison of the data is shown in Figure 3 of Perring et al.⁴⁴ During the BEARPEX 2009 field intensive in the Sierra Nevada Mountains in California, the Berkeley TD-LIF Σ AN measurements were made simultaneously with CIMS observations of specific nitrates for the first time. Beaver et al.⁵ found that the measured concentrations of INs, PROPNN, ETHLN, MVKN + MACRN, and MBON accounted for 65% of Σ ANs. The authors tentatively identified

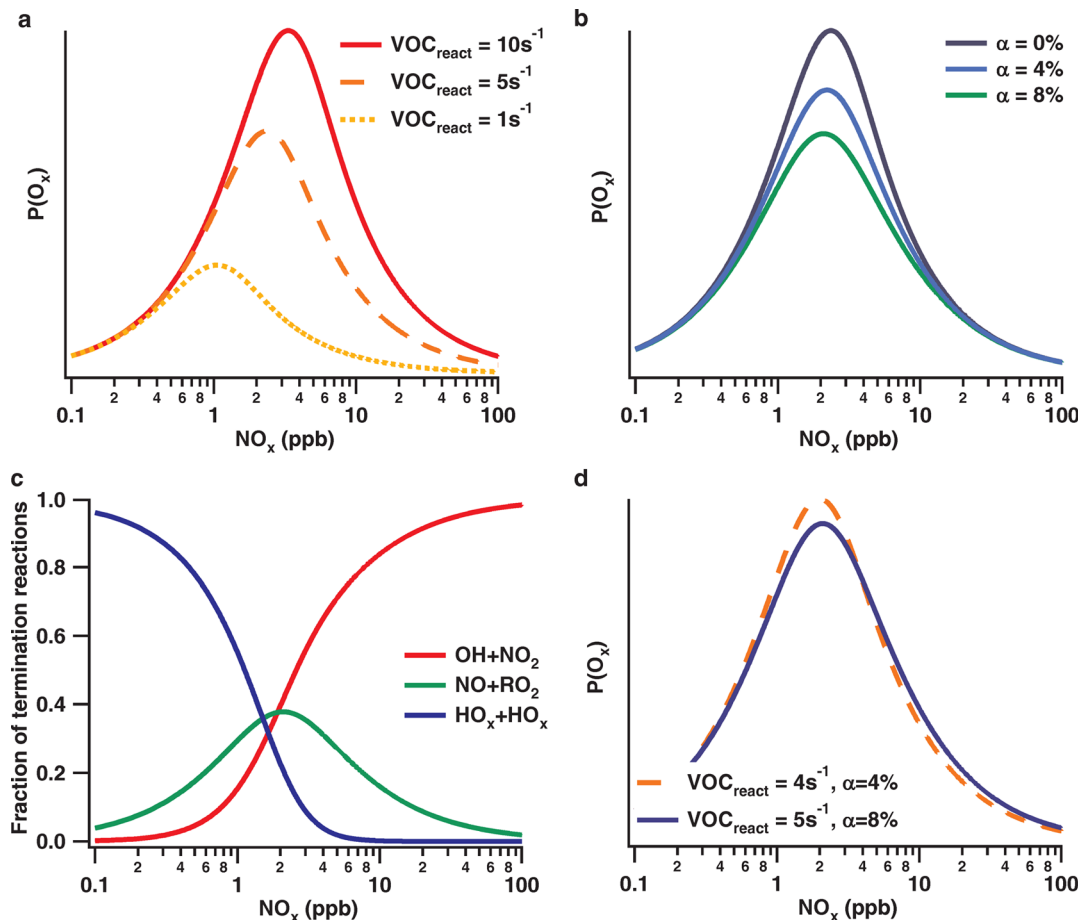


Figure 7. (a) $P(O_x)$ as a function of NO_x for an OH production rate of 10^6 molec/cm 3 /s and three different VOC reactivities: 10 s^{-1} (solid red line), 5 s^{-1} (dashed orange line), and 1 s^{-1} (dotted yellow line). (b) $P(O_x)$ as a function of NO_x for an OH production rate of 10^6 molecules/cm 3 /s and three different α values: 0% (dark blue), 4% (light blue), and 8% (green). (c) The relative importance of three possible chain termination reactions as a function of NO_x for a VOC reactivity of 5 s^{-1} and an OH production rate of 10^6 molec/cm 3 /s: formation of peroxydes (blue), formation of alkyl nitrates (green), and formation of HNO_3 (red). (d) Example of a scenario where a decrease of 20% in VOC reactivity, if accompanied by a decrease in α of 50%, can lead to an increase in $P(O_x)$. The blue line shows $P(O_x)$ if the VOC reactivity is 5 s^{-1} and $\alpha = 8\%$. The dashed orange line shows $P(O_x)$ if the VOC reactivity is reduced to 4 s^{-1} and α decreased to 4%.

four additional even m/z compounds and suggested the masses were consistent with assignment to $\text{NO}_3 +$ isoprene nitrate products (m/z 230 and 248) and NO_3 and OH-initiated α - or β -pinene oxidation nitrate products (m/z 316 and 300, respectively). After including these molecules in the summed speciated RONO_2 , their total was within 10% of $\sum\text{ANs}$ (Figure 6). Note that this implies that, at most, only a small fraction of the RONO_2 at UC-BFRS are dinitrates, which would thermally dissociate to give two NO_2 molecules for detection by TD-LIF.

The first in situ observations of $\sum\text{ANs}$ by the Berkeley TD-LIF were made at the University of California Blodgett Forest Research Station (UC-BFRS) in the Sierra Nevada Mountains where they were observed to be a much larger fraction of NO_y than the sum of individual RONO_2 from, until then, even the most comprehensive studies at other sites. In the summertime, they were observed to have a strong diurnal pattern with maximum concentrations (~ 500 ppt) occurring in the afternoon, and they represented $\sim 20\%$ of NO_y .⁸³ In the wintertime, they were a smaller fraction of NO_y , and concentrations of $\sum\text{ANs}$ were similar to background continental concentrations of the sum of individual RONO_2 seen at other northern hemisphere sites.¹¹⁷ $\sum\text{ANs}$ have also been measured at surface sites in Houston, TX,⁸² just outside of

Sacramento in Granite Bay, CA,⁸⁵ and in Mexico City.^{135,136} Observed median midday concentrations during summer were ~ 1.2 and ~ 1 ppb, corresponding to 11% and 10% of NO_y in Houston and Granite Bay, respectively.

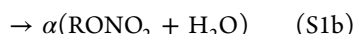
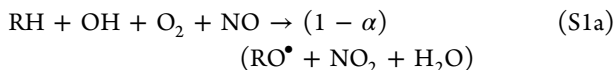
Perring et al.⁸⁶ reported the first airborne observations of $\sum\text{ANs}$ obtained during the NASA INTEX-NA campaign of 2004. Many flights occurred over the southeastern U.S., a region of high isoprene emissions, and calculations based on hydrocarbon observations indicated that isoprene was indeed the dominant $\sum\text{AN}$ precursor. When isoprene was high (>500 ppt), $\sum\text{ANs}$ were ~ 250 ppt and 18% of NO_y . A strong correlation was observed between $\sum\text{ANs}$ and formaldehyde (CH_2O), another product of isoprene oxidation. At that time, the concentrations of $\sum\text{ANs}$ described in the manuscript of 270 ppt (17% of NO_y) were significantly higher than the sum of all first-generation IN isomers previously observed in forested sites.^{42,110–112} Airborne observations of $\sum\text{ANs}$ were also made during the INTEX-B campaign of 2006, which included sampling in Mexico City, the Gulf of Mexico, and the remote Pacific. Concentrations of $\sum\text{ANs}$ in Mexico City were ~ 3 ppb and $\sim 10\%$ of NO_y near the city with the fraction increasing to $\sim 15\%$ downwind.¹³⁶ Concentrations of $\sum\text{ANs}$ over the Pacific were small (~ 20 pptv) and a minor fraction (<5%) of NO_y .

4. RONO₂ AND LOCAL O_x PRODUCTION

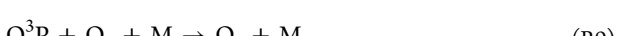
4.1. The Mechanistic Relationship between O_x and \sum ANs

The coupled HO_x and NO_x catalytic cycles that lead to the production of tropospheric O_x (O_x ≡ O₃ + NO₂) is used in this analysis because it is conserved under the fast but temporary titration of O₃ near NO sources, R8 and R9) and the primary termination products that limit the efficiency of these cycles are shown in Figure 1. The effects of NO on the conversion rate of RO₂ to HO₂ and of HO₂ to OH result in a nonlinear dependence of O_x production on the NO_x concentration (Figure 7a and b). At low NO_x, the HO_x cycle is primarily terminated via peroxide formation (Figure 1a). HO₂ and RO₂ reactions with NO are fast, yet at low NO levels peroxy radicals are only slowly converted to OH, thus resulting in both low OH concentrations and a low O_x production rate ($P(O_x)$). We note that for certain peroxy radicals (e.g., isoprene derived RO₂) there is an HO₂ + RO₂ channel that recycles OH coproducing RO and O₂; however, even for these species the presence of low to moderate NO will enhance OH and O_x production. At higher NO_x, HO₂ and RO₂ are more rapidly converted to OH, the oxidation of VOCs accelerates, $P(O_x)$ increases, and the dominant termination products result from HO_x-NO_x interactions (Figure 1b). The increases in OH and $P(O_x)$ are initially linear with NO_x, and the system is considered “NO_x-limited”. Beyond a certain point, further increases in NO_x result in a chemical mixture where NO₂ reacts with OH more rapidly than OH oxidizes organic molecules. In this “NO_x-saturated” and “VOC-limited” regime, HNO₃ is the dominant radical recombination product, and both the concentration of OH and $P(O_x)$ are suppressed. Chain termination by RONO₂ has its largest effect on HO_x and $P(O_x)$ at intermediate NO_x, and RONO₂ is the primary terminator for NO_x at low and intermediate NO_x abundances whenever organics larger than methane (CH₄) are important. Detailed discussions of the effects of RONO₂ formation on the HO_x cycle and $P(O_x)$ can be found in the literature;^{82,83,85,86,135,137,138} we summarize the major points below.

To understand the relationship between \sum ANs and O_x, we begin by writing their relative rates of production. The two rates are directly related by R3, and the balance between R3a and R3b is set by the nitrate branching ratio (α) (see section 2). Net production for O_x and \sum ANs from R1–R3a (for an alkane) is shown in condensed form in series 1a and 1b, respectively.

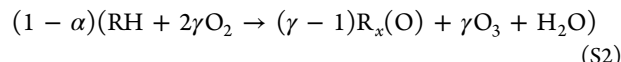


After RO[•] formation, the relevant reactions for $P(O_x)$ are:



The alkoxy radical typically reacts with O₂, producing a stable aldehyde or ketone and HO₂ (R6). HO₂ then reacts with NO, producing an additional NO₂ and regenerating OH. Photolysis of NO₂ results in an oxygen atom that combines with O₂ to

produce O₃. As noted in section 2.1, alkoxy radicals with a carbon backbone of 4 or more can also undergo isomerization or decomposition prior to reaction with O₂ generating, respectively, a hydroxyalkyl radical or a carbonyl and a smaller alkoxy radical. The alkyl or hydroxyalkyl radical then reacts with O₂ to form a peroxy radical, which interacts with NO via pathway 3a or 3b. This results in either an additional conversion of NO to NO₂ or the production of a nitrate, which would be multifunctional if generated from the isomerization reaction. Aschmann et al.¹³⁹ recently observed a yield of 5.4% of hydroxynitrates from the OH-initiated oxidation of *n*-octane. Note that because the formation of hydroxynitrates from the oxidation of alkanes has only been quantified for *n*-octane, these compounds are not included in the yields reported in Table 1. The effect of this chemistry is to increase total RONO₂ yields for long-chain alkanes in the above-reported values of simple alkyl nitrate yields. In addition, alkoxy radicals can decompose prior to reaction with O₂ generating a carbonyl and alkyl radical, which undergo subsequent reactions. While a complete discussion of specific VOC degradation schemes is beyond the scope of this Review, the relevant reaction mechanisms can be found in a review by Atkinson and Arey¹⁴⁰ and references therein. For the present purpose, a condensed form of these ozone producing chemical reactions R2, R3, and R6–R9 is given by series 2, where γ represents the number of O₃ produced and R_x represents the fact that each of the ($\gamma - 1$) carbonyl species may have a different hydrocarbon structure.



Typically, γ is 2. For CO and H₂CO, which have α equal to 0, γ is 1, and, if the hydrocarbon in question produces an additional peroxy radical by alkoxy radical isomerization rather than HO₂ plus a stable aldehyde or ketone, γ is 3 or more. Although $\gamma > 2$ for many C₄ and higher alkanes, for simplicity, we assume $\gamma = 2$ and S2 reduces to S3. The impacts of this assumption are discussed in the Appendix A.1 (Supporting Information).



Reactions R2, R3, and R6–R9 are generally fast with respect to R1, the initial reaction of the hydrocarbon with OH being the rate-limiting step. The instantaneous O_x and \sum AN production rates can therefore be written as weighted sums of the reaction rates of individual hydrocarbons with OH (eqs 1 and 2).

$$P(O_x) = \sum_i \gamma_i(1 - \alpha_i)k_{\text{OH}+\text{RH}_i}[\text{OH}][\text{RH}_i] \quad (1)$$

$$P(\sum \text{ANs}) = \sum_i \alpha_i k_{\text{OH}+\text{RH}_i}[\text{OH}][\text{RH}_i] \quad (2)$$

Taking the ratio of these two rates gives eq 3, where $\bar{\gamma}$ and $\bar{\alpha}$ are the OH reactivity-weighted means of the individual γ_i and α_i . This expression can be further simplified as shown below when $\bar{\alpha}$ is small and γ is 2 as is typically observed.

$$\frac{P(O_x)}{P(\sum \text{ANs})} = \frac{\bar{\gamma}(1 - \bar{\alpha})}{\bar{\alpha}} \approx \frac{2}{\bar{\alpha}} \quad (3)$$

Along with knowledge of the local VOC mixture, eqs 1–3 can be used to calculate the ratio of O_x to \sum AN production, or inverted (eq 4) to derive $\bar{\alpha}$ from estimates of $\bar{\gamma}$ and the O_x and \sum AN production rates. Typically, $P(O_x)$ is 10–100 times greater than $P(\sum \text{ANs})$, and $\bar{\alpha}$ is in the range of 1–10%.

$$\bar{\alpha} = \frac{\bar{\gamma}}{\frac{P(O_x)}{P(\sum ANs)} - \bar{\gamma}} \quad (4)$$

In what follows, we describe how eqs 3 and 4 have been used to interpret $\sum ANs$ observations, how this analysis is informative, and where it breaks down.

4.2. Observed Relationships between O_x and $\sum ANs$

Analyses of observed relationships between concentrations of $\sum ANs$, O_x , and other trace gases are often guided by the mechanistic frameworks of eqs 3 and 4. The challenge to this interpretation is that measured concentrations are only proxies for production rates. They are more accurate proxies (1) when photochemical production is rapid as compared to removal, chemistry, deposition, mixing across chemical gradients, and (2) when emissions of the precursor molecules, VOC and NO_x , are collocated. Interpreted through the lens of eqs 3 and 4, the slope of correlation of O_x versus $\sum ANs$ (Figure 8) gives the net

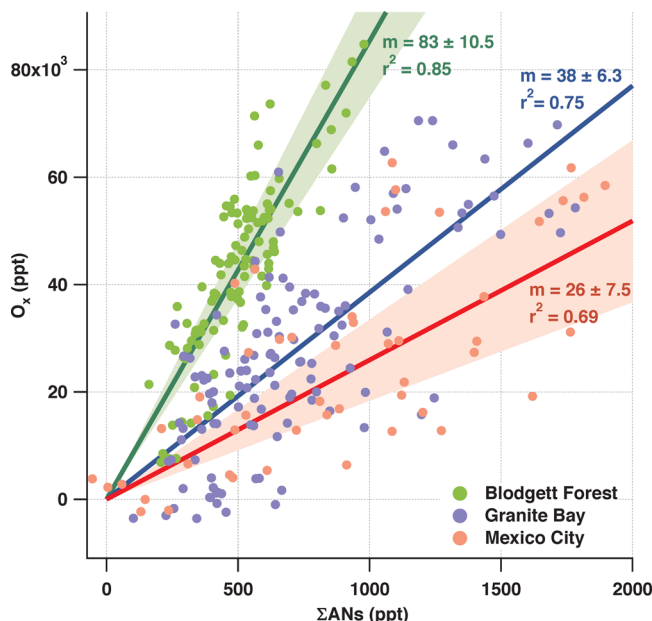


Figure 8. Example correlations between O_x and $\sum ANs$ for three different locations and NO_x regimes: UC-BFRS (Blodgett Forest), a rural location in the Western Sierra Nevada Mountains in CA (green); Granite Bay, a small city downwind of Sacramento, CA (blue); and Mexico City, a megacity (red). Solid lines show the best fit to the data, while shaded areas represent 2σ confidence bands. Granite Bay and Mexico City data are for 8 am to 2 pm local time. Blodgett forest is for August of 2001, in the afternoon between 2 pm and 6 pm, which, due to transport time, is thought to be reflective of chemistry taking place in Sacramento in the morning.

α of the entire VOC mixture. Differences between the $\alpha_{inferred}$ from this slope ($\alpha_{inferred}$) and that calculated by a summation over the observed VOC ($\alpha_{calculated}$) provide insights into both the amounts and the structures of unobserved VOC in a particular location. This is particularly useful, as incomplete characterization of VOCs remains one of the major analytical challenges in atmospheric chemistry, hindering our ability to understand how the atmosphere will respond to changes in climate and/or VOC emissions. In what follows, we discuss in more detail studies that have employed the above framework to interpret observations of $RONO_2$ and O_x .

In a recent experiment with ideal conditions for relating observed concentrations to production rates, Neuman et al.¹⁴¹ report on the correlation between O_x and $\sum RONO_2$ (measured as $NO_y-NO-NO_2-PAN-HNO_3$) in the outflow of the Deepwater Horizon (DWH) plume in the Gulf of Mexico in April 2010. The DWH plume was sampled in the daytime and consisted of extremely high abundances of large alkanes (such that production dominated loss), secondary oxidation products were a minimal fraction of the total VOC, and no other emissions sources were added to the chemical plume as it evolved (collocated emissions of precursor molecules). The authors showed that at each of four observed cross sections (10, 20, 30, and 50 km downwind), the O_x versus $\sum RONO_2$ slope was equal to the calculated ratio of $P(O_x)$ to $P(\sum ANs)$. For this plume, $\alpha_{calculated}$ and $\alpha_{inferred}$ were both $\sim 20\%$.

Figure 8 also shows the O_x versus $\sum ANs$ correlations observed at UC-BFRS in September of 2001⁸³ and Mexico City during March 2006.^{135,136} These urban and rural continental plumes are more challenging to interpret as chemicals are continually emitted into the plume as it evolves, the composition changes with time of day, and deposition becomes increasingly important. For example, disagreement between $\alpha_{inferred}$ and $\alpha_{calculated}$ is especially notable at UC-BFRS, and this is attributed to the fact that local biogenic emissions of high branching ratio VOC dominate $\alpha_{calculated}$ while the observed O_x is primarily transported from upwind near Sacramento where NO_x emissions are much higher. The $\alpha_{inferred}$ is therefore in large part controlled by the Sacramento area VOC, and thus NO_x and VOC sources at UC-BFRS are not collocated. That said, this analysis has yielded useful insights at these and other sites, each with different chemistries. $O_x/\sum ANs$ slopes, $\alpha_{inferred}$, $\alpha_{calculated}$ and the percent deviation of $\alpha_{calculated}$ from $\alpha_{inferred}$ for these two and additional locations are listed in Table 3. The

Table 3. O_x versus $\sum ANs$ Slope, Branching Ratios Inferred by That Correlation ($\alpha_{inferred}$), Average Branching Ratios Calculated from the Hydrocarbons ($\alpha_{calculated}$), and the Percent Deviation (Calculated as $(\alpha_{calculated} - \alpha_{inferred})/\alpha_{inferred}$) Tabulated for Six Different Locations

| | O_x vs $\sum ANs$ slope | inferred branching ratio ($\alpha_{inferred}$) | calculated branching ratio ($\alpha_{calculated}$) | % deviation ($(\alpha_{calculated} - \alpha_{inferred})/\alpha_{inferred}$) |
|-------------------|---------------------------|--|--|---|
| Houston | 41 | 4.7% | 4.5% | -4% |
| Granite Bay | 34 | 5.6% | 5.4% | -4% |
| Mexico City | 26 | 7.1% | 2.6% | -63% |
| southeastern U.S. | 59 | 3.3% | 5.1% | 55% |
| UC-BFRS | 80 | 2.4% | 10.6% | 342% |
| mid Pacific | 250 | 0.8% | 0.1 | -88% |

calculated $P(\sum ANs)$ for these sites are compared in Table 4, and a summary of the major classes of observed source VOCs at six locations is shown in Figure 9. Details of the calculations are presented in Appendix A.1 (Supporting Information).

We see from Figure 9 that organic $RONO_2$ precursors vary significantly by location. For example, BVOCs are more than 2/3 the source in both the southeastern U.S. and northern California. At two of these sites, the southeastern U.S. and Granite Bay, isoprene is the dominant BVOC, where at UC-BFRS, terpenes are the major local source. In larger urban regions, anthropogenic VOCs (primarily alkanes) are the dominant source, although alkenes are also significant in

Table 4. Tabulated OH Reactivity (OHr), $P(O_3)$, and $P(\sum ANs)$ for the Locations Discussed in the Text^a

| | C1–C5 alkanes | other alkanes | alkanes | isoprene +MACR +MVK | terpenes | aromatics | CO+ACAL +H ₂ CO | total |
|---------------|------------------|----------------|---------------|------------------------|---------------|----------------|-------------------------------|---------------|
| Houston | | | | | | | | |
| OHr | 0.79 | 0.95 (0.08) | 3.77 | 0.56 | 0.54 (0.39) | 0.66 (0.02) | 3.68 | 10.95 (0.49) |
| $P(O_3)$ | 0.24 | 0.28 (0.25) | 1.13 | 0.17 | 0.16 (0.12) | 0.2 (0.005) | 0.89 | 3.07 (0.15) |
| $P(\sum ANs)$ | 4.85 | 16.49 (1.44) | 15.9 | 6.61 | 18.48 (13.92) | 7.2 (0.28) | 0 | 69.63 (15.64) |
| Granite Bay | | | | | | | | |
| OHr | 0.33 | 0.2 (0.007) | 0.33 (0.029) | 2.44 | 0.14 (0.002) | 0.31 (0.05) | 2.39 (1.89) | 6.14 (1.98) |
| $P(O_3)$ | 0.097 | 0.06 (0.02) | 0.099 (0.009) | 0.73 | 0.042 (0.005) | 0.093 (0.0015) | 0.51 (0.28) | 1.63 (0.33) |
| $P(\sum ANs)$ | 0.8 | 3.82 (1.26) | 1.18 (0.088) | 30.11 | 4.81 (0.025) | 3.60 (0.88) | 0 | 44.32 (2.25) |
| Mexico City | | | | | | | | |
| OHr | 0.64 | 0.42 (0.031) | 0.7 | 0.06 | 0.018 (0.018) | 0.073 | 3.5 | 5.41 (0.049) |
| $P(O_3)$ | 0.2 | 0.13 (0.069) | 0.21 | 0.02 | 0.005 (0.005) | 0.02 | 0.75 | 1.34 (0.12) |
| $P(\sum ANs)$ | 3.17 | 7.7 (4.28) | 1.95 | 0.66 | 0.6 (0.6) | 0.7 | 0 | 14.78 (4.88) |
| SE U.S. | | | | | | | | |
| OHr | 0.31 | 0.039 (0.001) | 0.038 (0.020) | 1.19 | 0.042 (0.032) | 0.025 (0.021) | 1.57 | 3.21 (0.074) |
| $P(O_3)$ | 0.091 | 0.01 (0.007) | 0.011 (0.006) | 0.36 | 0.012 (0.009) | 0.008 (0.006) | 0.29 | 0.78 (0.028) |
| $P(\sum ANs)$ | 0.22 | 0.68 (0.49) | 0.18 (0.15) | 14.9 | 1.40 (1.07) | 0.32 (0.30) | 0 | 17.7 (2.01) |
| UC-BFRS | | | | | | | | |
| OHr | 0.29 (0.002) | 0.020 (0.014) | 0.079 (0.021) | 0.36 | 1.20 (0.007) | 0.025 (0.021) | 1.57 (0.92) | 3.77 (0.99) |
| $P(O_3)$ | 0.09 (0.001) | 0.006 (0.004) | 0.023 (0.006) | 0.11 | 0.36 (0.003) | 0.008 (0.006) | 0.29 | 0.89 (0.02) |
| $P(\sum ANs)$ | 0.15 (0.031) | 0.38 (0.31) | 0.21 (0.11) | 4.54 | 41.2 (0.13) | 0.32 (0.3) | 0 | 46.8 (0.88) |
| Pacific | | | | | | | | |
| OHr | 0.289 | 0.002 (0.0002) | 0.001 | 0 | 0 | 0.003 (0.001) | 0.918 | 1.213 (0.001) |
| $P(O_3)$ | 0.089 | 0.001 (0.0002) | 0.0004 | 0 | 0 | 0.001 (0.0002) | 0.16 | 0.25 (0.0004) |
| $P(\sum ANs)$ | 0.08 | 0.032 (0.011) | 0.001 | 0 | 0 | 0.022 (0.01) | 0 | 0.135 (0.021) |

^aThe first number in each box represents the total quantity for each class of compounds for a given location. The number in parentheses represents the quantity estimated for compounds for which there were no measurements. OHr is in s^{-1} , $P(O_3)$ is in ppb/h, and $P(\sum ANs)$ is in ppt/h. Note that both $P(O_3)$ and $P(\sum ANs)$ depend on the OH concentration. Production rates for all sites have been calculated using OH = 10^6 molecules/cm³ to normalize these values across sites with different OH concentrations and for which there are no measurements available. γ is assumed to be 2 for all hydrocarbons except CO and H₂CO for which it is 1 and CH₃CHO for which it is 3.

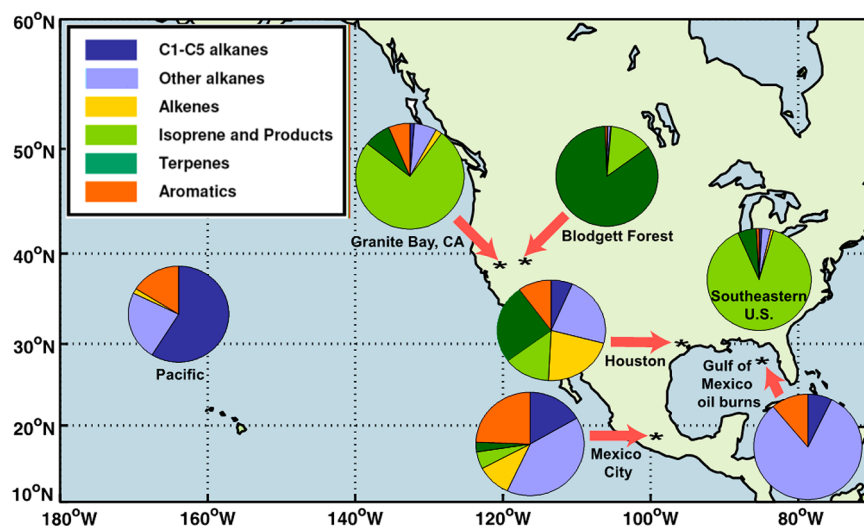


Figure 9. A map showing the distribution of source molecules in various locations where $\sum ANs$ have been measured. All locations are based on TD-LIF measurements except for the Gulf of Mexico oil burns where RONO₂ is inferred from NO_x, PAN, HNO₃, and NO_y measurements.

Houston and aromatics in Mexico City. Consistent with these source variations, the $O_x/\sum ANs$ slope is found to vary with location, by a factor of 5. The slope is also seen to vary with time of day increasing from morning to afternoon in suburban Granite Bay (35 to 50) and urban Houston (29 to 41), and with increased photochemical age in the Mexico City plume (17 to 90 over multiple days of processing). Both effects have been explained through increased RONO₂ deposition in the

afternoon, where RONO₂ deposition (~hours) is much faster than that of O₃ (~days), and increased oxidation later in the day of secondary oxidation products, such as CO and H₂CO, which produce O₃ but have an α of zero.⁸² Although the VOC mixture is also changing over time, favoring the retention of lower-reactivity (and often low α) compounds, the effects of this evolution on the $O_x/\sum ANs$ are expected to be much

smaller than those of deposition or secondary oxidation products.

Good agreement has been seen between α_{inferred} and α_{calc} ; for example, they agree to to 4% in both Houston and Granite Bay.^{82,85} Given both the approximations to the calculations (see section 4.1) and the estimates required to fill gaps in incomplete measurements of even those VOCs known to be important (Appendix A (Supporting Information)), this should be considered excellent agreement. In contrast, the discrepancy between α_{calc} and α_{inferred} for Mexico City (~62%) is much larger, indicating that more RONO₂ are produced per O₃ than can be explained by the presumed chemistry of the observed VOC. This is surprising as one expects urban VOCs to be the best-characterized sources, and the location satisfies both the requirements of rapid production relative to loss and collocated emission of precursor molecules. Therefore, the disagreement between α_{calc} and α_{inferred} is interpreted to be indicative of unknown elements in the photochemistry of Mexico City. Perring et al.¹³⁶ put forth three hypotheses to explain this difference in Mexico City: (1) the (highly uncertain) yield of aromatic RONO₂ is larger than currently assumed, (2) unmeasured, high- α VOCs are a larger portion of the reactivity than expected, and (3) RONO₂ themselves are a more important source than presumed to this reactivity.

Recently, Elrod³⁵ measured α for several aromatics showing that RONO₂ yields from the bicyclic peroxy radical intermediates of benzene, toluene, *p*-xylene, and 1,3,5-trimethylbenzene suggest overall α values that are smaller than those found in the Leeds Master Chemical Mechanism.¹⁴² This may rule out part of the aromatic hypothesis put forward by Perring et al.;¹³⁶ however, it is still possible that RONO₂ yields from ring-opening products are much higher. The second and third hypotheses are consistent with ideas put forward by Robinson et al.¹⁴³ who suggested there are sizable underestimates of $>\text{C}_{10}$ VOCs in urban emissions inventories (and observations). These VOCs would have high RONO₂ yields, of order 35%, and are large enough that it is likely that their nitrate products would have similarly high yields. It is commonly observed that the sum of the reactivities of individual VOCs and radicals underestimates total measured OH reactivities^{144–151} as such analysis of the O_x/ $\sum\text{ANs}$ slope is an additional constraint on what the missing OH reactivity in a given location may be.

Most published analyses have focused on the relationship between O_x and $\sum\text{ANs}$ when deposition and transport are minor effects. O_x/ $\sum\text{ANs}$ correlations are less informative in remote regions (e.g., in the Pacific Ocean) due to poorly constrained differential loss processes. Nonetheless, as discussed in section 5, $\sum\text{ANs}$ can remain a significant fraction (~10%) of NO_y even in the remote atmosphere, and, if NO_x and hydrocarbons are available at any level, there remains the possibility for their production. O_x and $\sum\text{ANs}$ correlations could be useful in analyses quantifying the impacts of transport and deposition in combination with Langrangian plume or other modeling studies, which incorporate a sufficiently detailed chemical mechanism.

4.3. Implications for Ozone Control Strategies and Models

RONO₂ production directly suppresses O_x production (via R3) and therefore has clear implications for air quality control strategies and atmospheric models. Figure 7 illustrates the sensitivities of peak P(O_x) to VOC and NO_x levels (Figure 7a and b, respectively). Figure 7c shows the relative importance of

chain termination reactions as a function of NO_x. This highlights that P($\sum\text{ANs}$) is maximized at intermediate NO_x concurrent with peak OH, but where OH is still reacting more frequently with VOCs than with NO₂. This is the same NO_x range where P(O_x) is maximized, rendering it especially important from an air quality management standpoint. The policy options for reducing O_x are to control NO_x emissions, VOC reactivity, or both. Under conditions of peak P(O_x), all three strategies are expected to decrease P(O_x). However, papers by Farmer et al.¹³⁵ and Perring et al.¹³⁶ demonstrate that the role of RONO₂ formation introduces complexity whereby changes in peak P(O_x) due to changes in VOC reactivity are dependent on the specific identity of the VOC(s) in question. A selective reduction of high- α VOCs, for example, might in fact increase P(O_x), while a selective reduction of low- α VOCs could suppress O₃ formation beyond the effect expected from just the change in reactivity. To illustrate these issues, Figure 7d shows that a 20% reduction in VOC emissions would decrease ozone production rates by 8% only if there were no change in the effective α . If this 20% reduction also decreased α from 8% to 4%, the effect would instead be to increase peak P(O_x) by 8%. We note that VOC control strategies have targeted high vapor pressure organics, but the larger, lower vapor pressure organics remaining almost certainly have higher α . This new understanding of the impact of RONO₂ can both inform future control strategies and lead to a more nuanced interpretation of why previous strategies have or have not worked as predicted by chemical transport models.

Such analyses require the development of chemical transport models with detailed RONO₂ production and loss mechanisms. These have only just become available,^{152,153} and, at present, most lack a detailed RONO₂ parametrization. Many are, however, now moving to include more complete isoprene chemistry.^{154–159} Regional models typically represent RONO₂ as a highly condensed and molecularly lumped category (for example, Carter et al.¹⁶⁰), even though RONO₂ fates vary widely depending on the structure of the nitrates and their precursors and do not include the temperature or pressure dependence of the RONO₂ formation mechanism. Browne and Cohen¹⁵³ have recently reported WRF-CHEM (Weather Research and Forecasting coupled to chemistry) model simulations of RONO₂ chemistry in low-NO_x environments using a detailed parametrization of isoprene nitrate formation and fate based on recent experimental results. They find that RONO₂ formation represents a larger instantaneous NO_x sink than does HNO₃ formation at NO_x levels below 400 pptv for an α of 5% and below 950 pptv for an α of 10%. In addition, for the lowest NO_x levels (10s of ppt), RONO₂ formation with an α of 10% decreases the NO_x lifetime by almost a factor of 3 and the ozone production efficiency by almost an order of magnitude. The NO_y speciation, NO_x lifetime, and ozone production efficiency are highly sensitive to the specific interactions between NO_x and different VOC's in ways that are location-specific and difficult to capture using lumped treatments. Model evaluations could be improved through assessment of not only their ability to reproduce NO_y speciation but also of their performance in reproducing observed correlations between O_x and $\sum\text{ANs}$.^{53,161,162}

In Figure 4, we illustrate potential degradation reactions of RONO₂ whereby some species may retain the nitrate functionality under subsequent oxidation while others may regenerate NO₂. The fraction of nitrate-retaining products (β as labeled in Figure 4) is compound specific as is the time scale for

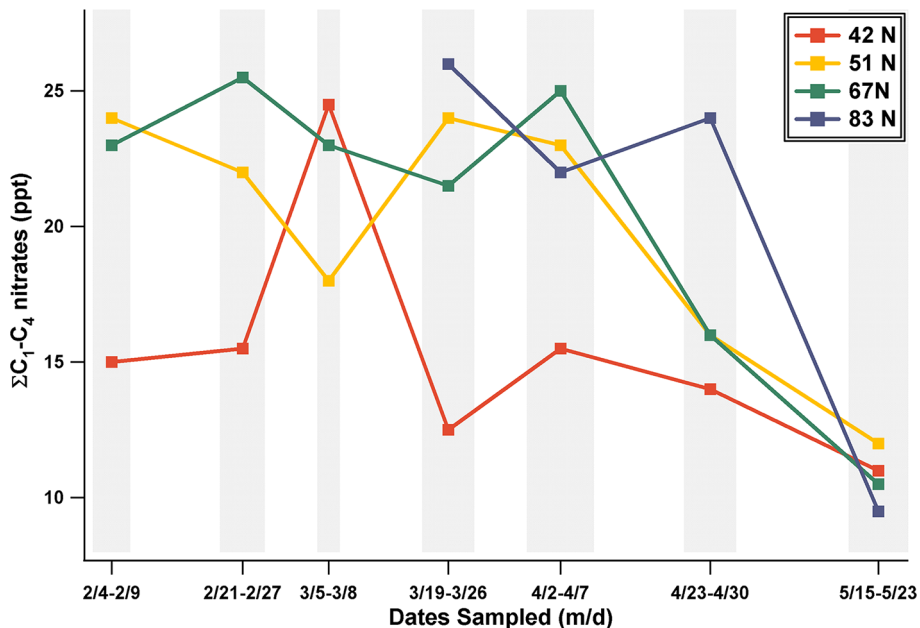


Figure 10. Adapted from Blake et al.¹⁶⁵ Shown are seasonal cycles of the sum of C₁–C₄ nitrates at four different latitudes sampled during the TOPSE campaign between February and May 2001. Shaded gray areas represent the windows of time over which samples were taken.

oxidation. It would be possible, for example, to have a molecule with a high α , which would significantly depress $P(O_x)$ in the near field, but a low β , such that it represents only a temporary NO_x sink. Such an RONO₂ would have an effect similar to a peroxy nitrate and would go on to contribute to $P(O_x)$ later in the plume evolution. In contrast, a compound with both high α and high β would depress $P(O_x)$ in the near field and be a more permanent NO_x sink. In summary, α sets the impact on local $P(O_x)$ near the point of emission, while β determines the permanence of NO_x sink by the RONO₂ formed. Note that the calculations presented in Figure 7 show the instantaneous effect of RONO₂ production near source regions on local $P(O_x)$ only. They are useful in guiding our thinking about the role of RONO₂. A calculation of the effect of RONO₂ chemistry on total $P(O_x)$ requires integration over time and accounting for transport and atmospheric mixing as can be achieved in a chemical transport model such as WRF-CHEM.^{153,163}

5. EXPORT OF RONO₂ AND NO_x ON REGIONAL TO GLOBAL SCALES

Many RONO₂ have significantly longer chemical lifetimes than NO_x. Consequently, they can be transported by winds and, upon oxidation, serve as a chemical source of NO_x at distances far removed from the initial emissions. RONO₂ are thus a potentially significant NO_x reservoir, affecting OH and O₃ on regional to global scales. For example, at the Alert research site (82° N), Muthuramu et al.¹⁶⁴ showed that C₃–C₇ nitrates, which were as much as 20% of the NO_y, could constitute an important NO_x source during polar sunrise. This class of RONO₂ has generally been observed to be a larger fraction of NO_y at high latitudes in the winter when decreased solar radiation leads to photochemical and photolytic lifetimes of months. The most geographically extensive measurements of RONO₂ in the remote atmosphere are those obtained during the TOPSE aircraft experiment. Blake et al.¹⁶⁵ described the seasonal and latitudinal trends of C₁–C₅ nitrates. The measurements (Figure 10) suggest that in the winter, the Northern Hemisphere can be characterized as two separate air

masses, midlatitude and polar, with occasional large-scale mixing events as seen in the March 5–8 observations, where midlatitude air appears at the pole and polar air in the mid latitudes. Seasonally, the sum of the individually measured RONO₂ at all latitudes began to decrease in early April with as much as 15 ppt either converted to NO_x or converted to multifunctional molecules by mid May. If it were assumed that all NO_x stored over the winter in RONO₂ form is released (which is an upper limit), the effect on the NO_x-limited atmosphere would be to significantly enhance local O₃ production. Similar conclusions have also been reached concerning the effects of oceanic CH₃ONO₂ emissions. Neu et al.¹⁶⁶ have shown that a model including oceanic emissions of methyl and ethyl nitrate, as observed by Chuck et al.¹¹ and Dahl et al.,¹⁶⁷ results in a 1 Dobson unit (~3%) enhancement in tropospheric columnar O₃.

Because of isoprene's abundance, INs are predicted to transfer more nitrogen from source regions than are all other RONO₂ species combined. Chen et al.³⁹ calculated that ~7% of the NO_x emitted in the northeastern U.S. is exported as INs. A number of other modeling and theoretical studies have also suggested that a substantial fraction of NO_y exported from North America is in the form of organic nitrates;^{168,169} however, these calculations remain largely unconfirmed by measurements or analysis of observations. Parrish et al.¹⁷⁰ found the majority (>60%) of exported NO_y is in the form of HNO₃. We interpret these results as implying that the RONO₂ reservoir is either lost to deposition or chemically converted to HNO₃ during transport. We note, however, that this study primarily involved air masses sampled near the coast of North America and that had undergone minimal cloud processing. We would therefore expect the importance of HNO₃, which should be preferentially removed by clouds, to be lower further downwind where wet removal has occurred.

Models have shown that both the magnitude and the sign of the impacts of IN export on global O₃ vary widely depending on the particular assumptions about branching between nitrate-retaining (β) and NO_x-releasing ($\beta - 1$) path-

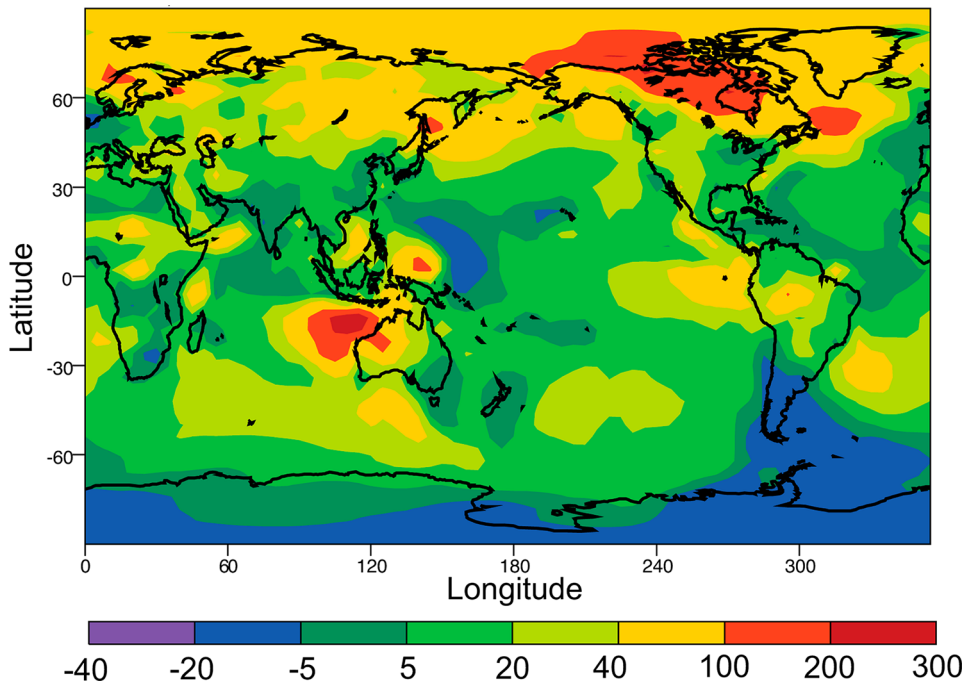


Figure 11. From Ito et al.¹³⁸ Spatial distribution of changes in surface NO_x resulting from the formation and transport of INs, which are then assumed, in this particular model, to regenerate NO_x.

ways.^{137,155,156,162,171–173} Models that treat INs as a permanent NO_x sink ($\beta = 1$) predict suppressed global ozone production (e.g., Fiore et al.¹⁷¹ and Wu et al.¹³⁷). The Wu study found that increasing α from the lowest published value of 4.4% to a higher yield of 12%³⁸ resulted in a ~10% decrease in the global tropospheric ozone burden. Von Kuhlman et al.¹⁷⁴ found that different isoprene oxidation mechanisms caused a spread of $\pm 35\%$ in the global O₃ burden attributed to isoprene. In models that treat INs as temporary NO_x reservoirs ($\beta < 1$), the overall effect of INs is analogous to that of peroxy nitrates (RO₂NO₂), where, through their transport and subsequent chemistry, RO₂NO₂ act as a NO_x source away from source regions. Figure 11 shows calculations of INs' impact (using $\beta < 1$) on global NO_x during July.¹³⁸ The authors show that almost everywhere on Earth NO_x is enhanced and, in many places, by more than 40%. Accordingly, this model predicts global O₃ increases due to IN chemistry. Simulations considering various β values by Paulot et al.¹⁵⁵ found that, in the tropics, the impact of INs on regional to global O₃ production was especially large as ~20% of isoprene emissions were oxidized above the boundary layer, where chemical lifetimes of RONO₂ were greatest.

Horowitz et al.⁵³ compared the 2004 INTEX-NA/ICARTT aircraft \sum AN data over the continental U.S. to a model calculation representing the range of possible production and recycling rates for INs. The authors found the data were best reproduced using an α of 4%, a nitrate-retaining efficiency (β) of ~50%, and a dry deposition rate similar to that of HNO₃, although the solution was not unique. Using these parameters, they calculated that 15–19% of NO_x emitted in the U.S. in summertime was consumed by IN formation. Of this total, 4–6% of the NO_x (~33% of the INs) cycled back to NO_x relatively quickly, 2–3% of the NO_x (~10% of the INs) was exported as INs, and 8–10% of the NO_x (~50% of the INs) was deposited to the surface. Perring et al.⁸⁶ took a different approach with the same \sum ANs data, examining the correlation of \sum ANs with CH₂O, both almost exclusively due to isoprene

oxidation in the data set. This analysis indicated that INs maintained their nitrate functionality through at least the first generation of oxidation and that the overall lifetime of INs to nitrate loss was significantly longer than the expected lifetime to oxidation. That study recommended the following paired values of α and β : [$\alpha = 4.4\%$, $\beta = 96\%$]; [$\alpha = 8\%$, $\beta = 84\%$]; [$\alpha = 12\%$, $\beta = 74\%$]. In a laboratory study using CIMS, Paulot et al.⁷ found an overall β of ~50% for INs but observed lifetimes and oxidation products that varied significantly for different IN isomers, such that some isomers regenerated NO_x on a relatively short time scale while others acted as longer-term NO_x reservoirs. Underscoring the importance of β in accurately capturing the impact of INs on regional scales, Xie et al.,¹⁵⁷ also with the 2004 INTEX-NA/ICARTT data set, found that uncertainties in β had greater impacts to measurement/model agreement than did uncertainties in α or rates of deposition.

6. RONO₂ AND SOA FORMATION

Organic molecules are a large fraction of total aerosol mass, and evidence suggests that most of this organic mass is formed by the atmospheric oxidation of VOCs, which creates lower volatility species that then partition into the aerosol phase.^{175–178} The gas- and aerosol-phase reactions that form secondary organic aerosol (SOA) are incompletely understood. SOA concentrations modeled with known mechanisms often dramatically underpredict observations (e.g., Volkamer et al.¹⁷⁹), and organic aerosol are often measured to have much higher oxygen:carbon than expected from the corresponding gas-phase reactions and rates (note that a nitrate group adds three oxygen per carbon). RONO₂ have been observed in SOA in the laboratory.^{51,66,67,180–189} Large multifunctional RONO₂ generated from OH-initiated oxidation of the alkanes and alkenes have been shown to readily partition to the aerosol phase. This is well described by models with known chemistry and standard gas-particle partitioning relationships for >C₁₄

hydrocarbons, but observations and calculations diverge as the carbon number decreases.⁶⁷

It is generally thought that OH-initiated SOA formation is favored at low NO_x, where peroxides are the dominant chain termination products as ROOH molecules themselves have reduced vapor pressures and are susceptible to chemical reactions within aerosol that prevent repartitioning to the gas phase. At higher NO_x, reactions between RO₂ + NO are most important and mass yields are seen to decrease; that said, SOA yields specifically from RONO₂ are not monitored in these experiments.^{190–193}

RONO₂ formed from NO₃-initiated oxidation are at least doubly functionalized, and the volatility change from the parent molecule is more substantial. SOA yields for reactions between NO₃ and key BVOCs have been reported from chamber studies. NO₃ oxidation of isoprene has been observed to lead to SOA production with modest yields and is thought to be an important SOA source.^{51,193} Higher yields have been observed for β-pinene, limonene, and other terpenes, implying terpene-derived RONO₂ may be an especially significant global SOA source.^{43,182} In a modeling study, Hoyle et al.¹⁹⁴ found that in urban areas 50–60% of near surface SOA may be due to NO₃-initiated oxidation during evening hours.

There are limited ambient observations of either speciated or total RONO₂ in the aerosol phase available. Measurements have been made at a number of field sites using Fourier transform infrared (FTIR) spectroscopy,^{88,195–200} with electrospray ionization mass spectrometric techniques (ESI-MS),^{200–206} and to a limited extent by aerosol mass spectrometry (AMS).^{207,208} Recently, the first ambient measurements by the Berkeley TD-LIF of aerosol-phase ΣANs have been reported.²⁰⁹

FTIR quantifies the number of nitrate functional groups and is calibrated with a set of RONO₂ standards. The absorbance at 1260–1280 cm⁻¹ is generally preferred due to its sharpness, intensity, and freedom from interferences.^{180,195,198,199,210} FTIR is an off-line technique and the time resolution defined by the frequency of the filter collection, which is typically hourly to daily. FTIR measurements from the Scripps Pier in San Diego, CA, show the mass of the nitrate group composed up to 10% of the total organic mass in submicrometer particles and that these groups were more prevalent in polluted urban air masses.^{195,199}

Often preceded by liquid chromatographic separation, ESI-MS has been used to identify and to quantify (but only for a subset of molecules using surrogate standards) a variety of nitrooxy organosulfates in ambient aerosol.^{200–206,211,212} This technique has been applied to organic matter in rain^{213–215} and fogwater samples.²⁰⁰ Also an off-line technique, this method is unique in that it gives information on the R group and thus the specific nitrate VOC precursor; however, mass identification is nontrivial. The nitrooxy organosulfates that are observed are often derived from isoprene and α-pinene and as a result are considered markers for biogenic influence on SOA formation. Enhancements in nitrooxy organosulfates have been seen in nighttime samples at field sites across Europe.^{201,202,212} This has been interpreted as evidence of the importance of NO₃-driven chemistry to SOA formation, a point supported by laboratory observations with H₂SO₄ seed aerosol under both intermediate and high NO_x conditions.²⁰⁴

AMS is widely used to quantify the organic component of aerosol^{177,216–219} and specific subsets of this portion,^{143,179,220–224} and is capable of high-time resolution observations. Chamber studies indicate that upon ionization

RONO₂ produce NO⁺ and NO₂⁺, the same fragments, although in a different ratio, as inorganic nitrate (NO₃⁻). In the laboratory, Fry et al.⁴³ studied aerosol RONO₂ chemistry by AMS in an NO₃⁻ free environment, and Bruns et al.²⁰⁷ did so by monitoring the change in the NO₂⁺:NO⁺ fragmentation ratio. In the field, Bae et al.²²⁵ inferred the presence of organic nitrates in particles by the NO₂⁺:NO⁺ at a rural site in southwestern New York. Farmer et al.²⁰⁸ tested five methods of quantifying aerosol RONO₂ in ambient AMS data from Riverside, CA during SOAR-1 in 2005: the NO₂⁺:NO⁺ ratio, the fragmentation to HNO₃⁺ ions, fragmentation to C_xH_yO_zN⁺ organic ions, the NH₄⁺ balance, and the difference between the total and inorganic NO₃⁻. Ultimately, the authors cautiously estimated organic nitrates comprised 5–10% of the total nitrate aerosol mass.

Rollins et al.⁵¹ recently reported a Berkeley TD-LIF instrument targeting particulate phase ΣANs (pΣANs). Through a series of SOA flow tube experiments, the authors demonstrated TD-LIF to be both capable of fast aerosol sampling (~seconds) and specificity to the RONO₂ functional group (no NO₃⁻ interference). This Berkeley TD-LIF system is operated as described in section 2.2 with the exception that all gas-phase species are first removed using an activated carbon denuder. The air is then pulled through the heated oven (~350 °C) where aerosols are volatilized and RONO₂ compounds thermally dissociated. TD-LIF has the potential to be a useful tool for ambient pΣAN detection as aerosol, and gas-phase ΣANs can be measured simultaneously giving new insight into RONO₂ partitioning. Ambient observations using this technique were made in Bakersfield, CA in 2010.²⁰⁹ The authors observed a rapid increase in the pΣANs fraction of organic aerosol (measured by AMS) from 6:30–11:30 pm corresponding to active nighttime NO₃ radical chemistry (Figure 12). These data serve as the first direct evidence for a large mass contribution to SOA by RONO₂ produced by NO₃ radical oxidation. During this time period, the authors found that the mass of the -ONO₂ functional group accounted for ~10% of the total organic aerosol. The authors went on to speculate that, if the molecules making up this mass had an average molecular weight of 200–300 g/mol, then 27–40% of the organic aerosol mass was attributable to RONO₂ molecules. Moreover, they found that the production of pΣANs, defined as the concentration difference between 6:30–11:30 pm, was greater when the VOC reactivity to NO₃ was smaller, likely driven by lower BVOC abundances. This implies that at lower VOC reactivities NO₃-initiated chemistry produces more multiply oxidized products with lower vapor pressures than their singly oxidized analogs. Aerosol-phase RONO₂ in Bakersfield, CA are therefore likely to be at least dinitrates. The production of pΣAN was also seen to vary linearly with the calculated NO₃ production rate ($k_{\text{NO}_2+\text{O}_3}[\text{NO}_2][\text{O}_3]$), suggesting that NO₃ was the limiting reagent. Although the VOCs may be biogenic, NO_x is predominantly not, suggesting that particulate RONO₂ and thus total aerosol loadings would decrease with NO_x emissions controls.

The role of RONO₂ in SOA chemistry is also affected by liquid-phase reactions within particles that occur at typically observed acidities and on SOA-relevant time scales. Laboratory studies with bulk solutions have shown tertiary RONO₂ readily hydrolyze, particularly at low pH, losing the nitrate moiety to produce alcohols and, when the acid catalyst is sulfuric acid, to produce organosulfates.^{203,226–229} Lui et al.²³⁰ recently studied RONO₂ hydrolysis in neutral aerosol in a reaction chamber

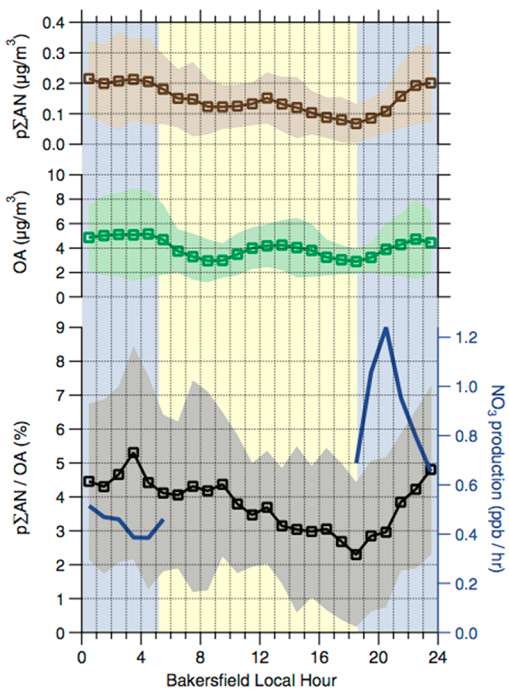


Figure 12. From Rollins et al.²⁰⁹ Here, $p\sum\text{ANs}$ (brown), OA (green), $p\sum\text{ANs}/\text{OA}$ (black), and NO_3 production rate (blue) are shown versus time of day (means with $\pm 1\sigma$ shaded). Nighttime (solar zenith angle $>85^\circ$) and daytime are shown in blue and yellow, respectively.

with 1,2,4-trimethylbenzene (TMB) SOA (TMB forms tertiary nitrates). They observed a strong relationship between aerosol RONO₂ loss and relative humidity. The authors found that, although nitrates may initially comprise up to 20% of organic aerosol, the nitrate mass fraction decreased substantially when RH > 20% and decreased at faster rates with higher RH (by a factor of 2–4). Ambient data support aerosol-phase loss of RONO₂,¹⁹⁵ and, as a result, the true RONO₂ contribution to SOA may be underestimated, particularly when observations are collected from filters with long integrated sampling times. Working in the opposite direction, experiments have also shown that RONO₂ can be formed in particles by addition reactions combining isoprene-derived epoxy diols and NO₃[−] nucleophiles.^{227,231–233}

7. CONCLUSIONS AND RECOMMENDATIONS FOR FUTURE WORK

Over a decade of ambient measurements of individual RONO₂ and $\sum\text{ANs}$ have brought about a variety of valuable insights into the chemistry of the Earth's atmosphere. Important findings described in this Review include:

- Confirmation that RONO₂ are ubiquitous in the boundary layer, that they are a major fraction of total reactive nitrogen oxides in both urban and rural chemical regimes and in diverse hydrocarbon mixtures, and that $\sum\text{ANs}$ are most often complex multifunctional species that remain difficult to observe by chromatography at ambient abundances. A subset of these multifunctional RONO₂ can now be observed by CIMS at atmospheric concentrations.
- A description of the role of RONO₂ as a free radical chain termination product of nearly equal importance to peroxides and HNO₃ at intermediate NO_x levels and the effect of RONO₂ on peak O₃ production rates on local to global scales.

- An exploration of the constraints observed $\sum\text{ANs}$ can provide on the chemical properties of VOC mixtures in different chemical regimes including highlighting unknown organic reactivity by deriving the net RONO₂ yield.

- An increasingly detailed understanding of formation and fates of INs and the special chemistry of isoprene, the single most important VOC emitted to the atmosphere.

- Recognition of the importance of including RONO₂ in regional and global models and of accurately tracking the transformation and fate of RONO₂ through multiple generations of oxidation.

Many important questions remain, and to conclude we present a selection of recommendations for future work:

- What are the rates of chemical, physiological (e.g., uptake into plant stomata),²³⁴ and physical (deposition onto wet and dry surfaces) removal of $\sum\text{ANs}$ and individual RONO₂?

- Are RONO₂ a major source of secondary organic aerosol in many different locations? Will or have NO_x emissions reductions affected the contribution of RONO₂ to total aerosol concentrations?

- How does a more detailed and quantitative description of RONO₂ chemistry in chemical transport models improve predictions such as the efficacy of emissions controls aimed at reducing human and agricultural exposure to unhealthy levels of O₃ and aerosol?

- Does inclusion of RONO₂ chemistry alter calculations of the preindustrial O₃ and aerosol against which we measure their present-day and future climate impacts and responses?

We look forward to new laboratory and field observations and to the development and evaluation of both modeling approaches and new analytical tools for ambient gas- and aerosol-phase RONO₂ measurements. We believe these will lead to more reliable predictions of O₃ and SOA, to more effective strategies for improving air quality and quantifying climate forcing, and to a more comprehensive understanding of the atmospheric chemistry of urban, suburban, and remote regions among other interesting questions.

ASSOCIATED CONTENT

Supporting Information

Appendix. This material is available free of charge via the Internet at <http://pubs.acs.org>.

AUTHOR INFORMATION

Corresponding Author

*E-mail: rccohen@berkeley.edu.

Present Addresses

[§]National Oceanic and Atmospheric Administration, Earth System Research Laboratory, Chemical Sciences Division, Boulder, Colorado 80305, United States.

[¶]University of Colorado, Cooperative Institute for Research in Environmental Sciences, Boulder, Colorado 80309, United States.

Notes

The authors declare no competing financial interest.

Biographies



Anne E. Perring received her B.S. in Chemistry from Brown University (2003) where she worked under Professors James Baird and Yongsong Huang. She performed her doctoral work at the University of California, Berkeley under the supervision of Ronald Cohen. In her research, she investigated the impacts of alkyl- and multifunctional nitrate formation on local and regional ozone and NO_x through the use of aircraft-based and laboratory studies. After receiving her Ph.D. in the summer of 2009 she became a Research Scientist at the National Oceanic and Atmospheric Administration in Boulder, CO, where she now focuses on the role of black carbon aerosol in the global atmosphere.



Sally E. Pusede is a graduate student in Physical Chemistry at the University of California Berkeley with Ronald Cohen. Her work focuses on using ambient measurements made at the surface and from aircraft to enhance our understanding of urban photochemistry, particularly the impacts of NO_x and organic emissions reductions on ozone and aerosol.



Ronald C. Cohen earned a B.A. with High Honors from Wesleyan University (1985), and a Ph.D. in Chemistry, from UC Berkeley (1991) working on high resolution spectroscopy of molecular clusters and radicals. As a postdoctoral fellow and the research associate at Harvard University 1991–1996 with Prof. James G. Anderson, he studied the photochemistry of the stratosphere. He joined the UC Berkeley faculty in 1995 where he is Professor and Vice Chair of Chemistry, Professor of Earth and Planetary Science Departments, and Director of the Berkeley Atmospheric Science Center. He is a faculty scientist in the Energy and Environment Division at the Lawrence Berkeley National. He is a Fellow of the American Geophysical Union (2012). Cohen's research combines satellite, in situ, and laboratory observations aimed at understanding the role of chemical reactions have in the Earth's climate and the chemistry producing unhealthy levels of ozone and fine particles. His research focuses on nitrogen oxide chemistry and the exchange of nitrogen oxides with ecosystems using laboratory, in situ, and satellite-based observations on the chemistry of evaporation/condensation with an eye toward understanding cloud formation and the long-term record of water isotopes recorded in the ice sheets of Greenland and Antarctica. He is leading a new effort to build analytic instruments for observing urban greenhouse gas emissions with unprecedented spatial resolution; see www.beacon.berkeley.edu.

ACKNOWLEDGMENTS

Research on organic nitrates at Berkeley has been funded by NASA headquarters under the Earth Systems Science Fellowship Program to AEP, and by NASA grants NNG05GH196, NAG5-13668, and NNX08AES6G and by NSF grants ATM-0639847 and ATM-0511829.

ABBREVIATIONS

| | |
|----------------------------|--|
| UC-BFRS | University of California-Blodgett Forest Research Station |
| VOC | volatile organic compound |
| BVOC | biogenic volatile organic compound |
| \sum ANs | total RONO ₂ as measured by TD-LIF |
| \sum PNs | total RO ₂ NO ₂ as measured by TD-LIF |
| p \sum ANs | total aerosol-phase RONO ₂ as measured by TD-LIF |
| TD-LIF | thermal dissociation-laser induced fluorescence |
| AMS | aerosol mass spectrometry |
| ESI | electrospray ionization |
| LC | liquid chromatography |
| MS | mass spectrometry |
| PTR-MS | proton transfer reaction-mass spectrometry |
| CIMS | chemical ionization mass spectrometry |
| PROPN | propanone nitrate |
| ETHLN | ethanal nitrate |
| MVKN | methyl vinyl ketone nitrate |
| MACRN | methacrolein nitrate |
| MBO | 2-methyl-3-buten-2-ol |
| MBON | MBO nitrate |
| SOA | secondary organic aerosol |
| IN | isoprene nitrate |
| TD-CRDS | thermal dissociation-cavity ringdown spectroscopy |
| α_{inferred} | RONO ₂ inferred from the correlation of O _x versus ANs |
| α_{calc} | RONO ₂ branching ratio calculated from measured VOCs |

REFERENCES

- (1) Pope, C. A.; Dockery, D. W. *J. Air Waste Manage. Assoc.* **2006**, *56*, 709.
- (2) Clarke, A.; Kapustin, V. *Science* **2010**, *329*, 1488.
- (3) Kanakidou, M.; Seinfeld, J. H.; Pandis, S. N.; Barnes, I.; Dentener, F. J.; Facchini, M. C.; Van Dingenen, R.; Ervens, B.; Nenes, A.; Nielsen, C. J.; Swietlicki, E.; Putaud, J. P.; Balkanski, Y.; Fuzzi, S.; Horth, J.; Moortgat, G. K.; Winterhalter, R.; Myhre, C. E. L.; Tsigaridis, K.; Vignati, E.; Stephanou, E. G.; Wilson, J. *Atmos. Chem. Phys.* **2005**, *5*, 1053.
- (4) Day, D. A.; Wooldridge, P. J.; Dillon, M. B.; Thornton, J. A.; Cohen, R. C. *J. Geophys. Res.: Atmos.* **2002**, DOI: 10.1029/2001JD000779.
- (5) Beaver, M. R.; St Clair, J. M.; Paulot, F.; Spencer, K. M.; Crounse, J. D.; LaFranchi, B. W.; Min, K. E.; Pusede, S. E.; Wooldridge, P. J.; Schade, G. W.; Park, C.; Cohen, R. C.; Wennberg, P. O. *Atmos. Chem. Phys.* **2012**, *12*, 5773.
- (6) D'Anna, B.; Wisthaler, A.; Andreasen, O.; Hansel, A.; Hjorth, J.; Jensen, N. R.; Nielsen, C. J.; Stenstrom, Y.; Viidanoja, J. *J. Phys. Chem. A* **2005**, *109*, 5104.
- (7) Paulot, F.; Crounse, J. D.; Kjaergaard, H. G.; Kroll, J. H.; Seinfeld, J. H.; Wennberg, P. O. *Atmos. Chem. Phys.* **2009**, *9*, 1479.
- (8) Roberts, J. M. *Atmos. Environ., Part A* **1990**, *24*, 243.
- (9) Shepson, P. B. In *Volatile Organic Compounds in the Atmosphere*; Koppmann, R., Ed.; Blackwell Publishing: Oxford, 2007.
- (10) Atlas, E.; Pollock, W.; Greenberg, J.; Heidt, L.; Thompson, A. M. *J. Geophys. Res.: Atmos.* **1993**, *98*, 16933.
- (11) Chuck, A. L.; Turner, S. M.; Liss, P. S. *Science* **2002**, *297*, 1151.
- (12) Talbot, R. W.; Dibb, J. E.; Scheuer, E. M.; Bradshaw, J. D.; Sandholm, S. T.; Singh, H. B.; Blake, D. R.; Blake, N. J.; Atlas, E.; Flocke, F. *J. Geophys. Res.: Atmos.* **2000**, *105*, 6681.
- (13) Blake, N. J.; Blake, D. R.; Wingenter, O. W.; Sive, B. C.; Kang, C. H.; Thornton, D. C.; Bandy, A. R.; Atlas, E.; Flocke, F.; Harris, J. M.; Rowland, F. S. *J. Geophys. Res.: Atmos.* **1999**, *104*, 21803.
- (14) Aschmann, S. M.; Atkinson, R.; Arey, J. *J. Geophys. Res.: Atmos.* **2002**, DOI: 10.1029/2001jd001098.
- (15) Capouet, M.; Muller, J. F. *Atmos. Chem. Phys.* **2006**, *6*, 1455.
- (16) Noziere, B.; Barnes, I.; Becker, K. H. *J. Geophys. Res.: Atmos.* **1999**, *104*, 23645.
- (17) Matsunaga, A.; Ziemann, P. J. *Proc. Natl. Acad. Sci. U.S.A.* **2010**, *107*, 6664.
- (18) Zhao, J.; Zhang, R. Y.; Fortner, E. C.; North, S. W. *J. Am. Chem. Soc.* **2004**, *126*, 2686.
- (19) Roberts, J. M. In *Volatile Organic Compounds in the Atmosphere*; Koppmann, R., Ed.; Blackwell Publishing: Oxford, 2007.
- (20) Atkinson, R.; Aschmann, S. M.; Carter, W. P. L.; Winer, A. M.; Pitts, J. N. *J. Phys. Chem.* **1982**, *86*, 4563.
- (21) Arey, J.; Aschmann, S. M.; Kwok, E. S. C.; Atkinson, R. *J. Phys. Chem. A* **2001**, *105*, 1020.
- (22) O'Brien, J. M.; Czuba, E.; Hastie, D. R.; Francisco, J. S.; Shepson, P. B. *J. Phys. Chem. A* **1998**, *102*, 8903.
- (23) Atkinson, R.; Carter, W. P. L.; Winer, A. M. *J. Phys. Chem.* **1983**, *87*, 2012.
- (24) Butkovskaya, N.; Kukui, A.; Le Bras, G. *J. Phys. Chem. A* **2010**, *114*, 956.
- (25) Butkovskaya, N. I.; Kukui, A.; Le Bras, G. *Z. Phys. Chem.* **2010**, *224*, 1025.
- (26) Cassanelli, P.; Fox, D. J.; Cox, R. A. *Phys. Chem. Chem. Phys.* **2007**, *9*, 4332.
- (27) Aschmann, S. M.; Long, W. D.; Atkinson, R. *J. Phys. Chem. A* **2006**, *110*, 6617.
- (28) Chow, J. M.; Miller, A. M.; Elrod, M. J. *J. Phys. Chem. A* **2003**, *107*, 3040.
- (29) Harris, S. J.; Kerr, J. A. *Int. J. Chem. Kinet.* **1989**, *21*, 207.
- (30) Elrod, M. J.; Scholtens, K. W.; Messer, B. M.; Cappa, C. D. *Abstr. Pap. Am. Chem. Soc.* **1999**, *217*, U363.
- (31) Lohr, L. L.; Barker, J. R.; Shroll, R. M. *J. Phys. Chem. A* **2003**, *107*, 7429.
- (32) Ellison, G. B.; Herbert, J. M.; McCoy, A. B.; Stanton, J. F.; Szalay, P. G. *J. Phys. Chem. A* **2004**, *108*, 7639.
- (33) Atkinson, R.; Aschmann, S. M.; Arey, J. *Int. J. Chem. Kinet.* **1991**, *23*, 77.
- (34) Atkinson, R.; Aschmann, S. M.; Arey, J.; Carter, W. P. L. *Int. J. Chem. Kinet.* **1989**, *21*, 801.
- (35) Elrod, M. J. *J. Phys. Chem. A* **2011**, *115*, 8125.
- (36) Guenther, A.; Karl, T.; Harley, P.; Wiedinmyer, C.; Palmer, P. I.; Geron, C. *Atmos. Chem. Phys.* **2006**, *6*, 3181.
- (37) Tuazon, E. C.; Atkinson, R. *Int. J. Chem. Kinet.* **1990**, *22*, 1221.
- (38) Sprengnether, M.; Demerjian, K. L.; Donahue, N. M.; Anderson, J. G. *J. Geophys. Res.: Atmos.* **2002**, DOI: 10.1029/2001JD000716.
- (39) Chen, X. H.; Hulbert, D.; Shepson, P. B. *J. Geophys. Res.: Atmos.* **1998**, *103*, 25563.
- (40) Patchen, A. K.; Pennino, M. J.; Kiep, A. C.; Elrod, M. J. *Int. J. Chem. Kinet.* **2007**, *39*, 353.
- (41) Lockwood, A. L.; Shepson, P. B.; Fiddler, M. N.; Alaghmand, M. *Atmos. Chem. Phys.* **2010**, *10*, 6169.
- (42) Giacopelli, P.; Ford, K.; Espada, C.; Shepson, P. B. *J. Geophys. Res.: Atmos.* **2005**, DOI: 10.1029/2004JD005123.
- (43) Fry, J. L.; Kiendler-Scharr, A.; Rollins, A. W.; Wooldridge, P. J.; Brown, S. S.; Fuchs, H.; Dube, W.; Mensah, A.; dalMaso, M.; Tillmann, R.; Dorn, H. P.; Brauers, T.; Cohen, R. C. *Atmos. Chem. Phys.* **2009**, *9*, 1431.
- (44) Perring, A. E.; Wisthaler, A.; Graus, M.; Wooldridge, P. J.; Lockwood, A. L.; Mielke, L. H.; Shepson, P. B.; Hansel, A.; Cohen, R. C. *Atmos. Chem. Phys.* **2009**, *9*, 4945.
- (45) Spittler, M.; Barnes, I.; Bejan, I.; Brockmann, K. J.; Benter, T.; Wirtz, K. *Atmos. Environ.* **2006**, *40*, S116.
- (46) Shepson, P. B.; Edney, E. O.; Kleindienst, T. E.; Pittman, J. H.; Namie, G. R.; Cupitt, L. T. *Environ. Sci. Technol.* **1985**, *19*, 849.
- (47) Hjorth, J.; Lohse, C.; Nielsen, C. J.; Skov, H.; Restelli, G. *J. Phys. Chem.* **1990**, *94*, 7494.
- (48) Barnes, I.; Bastian, V.; Becker, K. H.; Tong, Z. *J. Phys. Chem.* **1990**, *94*, 2413.
- (49) Wangberg, I. *J. Atmos. Chem.* **1993**, *17*, 229.
- (50) Berndt, T.; Boge, O. *Int. J. Chem. Kinet.* **1997**, *29*, 755.
- (51) Rollins, A. W.; Kiendler-Scharr, A.; Fry, J. L.; Brauers, T.; Brown, S. S.; Dorn, H. P.; Dube, W. P.; Fuchs, H.; Mensah, A.; Mentel, T. F.; Rohrer, F.; Tillmann, R.; Wegener, R.; Wooldridge, P. J.; Cohen, R. C. *Atmos. Chem. Phys.* **2009**, *9*, 6685.
- (52) Atkinson, R.; Aschmann, S. M.; Arey, J. *Environ. Sci. Technol.* **1992**, *26*, 1397.
- (53) Horowitz, L. W.; Fiore, A. M.; Milly, G. P.; Cohen, R. C.; Perring, A.; Wooldridge, P. J.; Hess, P. G.; Emmons, L. K.; Lamarque, J. F. *J. Geophys. Res.: Atmos.* **2007**, DOI: 10.1029/2006JD007747.
- (54) Skov, H.; Hjorth, J.; Lohse, C.; Jensen, N. R.; Restelli, G. *Atmos. Environ., Part A* **1992**, *26*, 2771.
- (55) Wangberg, I.; Barnes, I.; Becker, K. H. *Environ. Sci. Technol.* **1997**, *31*, 2130.
- (56) Aschmann, S. M.; Tuazon, E. C.; Arey, J.; Atkinson, R. *Atmos. Environ.* **2011**, *45*, 1695.
- (57) Aschmann, S. M.; Arey, J.; Atkinson, R. *Atmos. Environ.* **2012**, *46*, 264.
- (58) Kames, J.; Schurath, U. *J. Atmos. Chem.* **1992**, *15*, 79.
- (59) Fischer, R. G.; Ballschmiter, K. *Chemosphere* **1998**, *36*, 2891.
- (60) Shepson, P. B.; Mackay, E.; Muthuramu, K. *Environ. Sci. Technol.* **1996**, *30*, 3618.
- (61) Treves, K.; Shragina, L.; Rudich, Y. *Environ. Sci. Technol.* **2000**, *34*, 1197.
- (62) Seinfeld, J. H.; Pandis, S. N. *Atmospheric Chemistry and Physics*, 2nd ed.; John Wiley & Sons, Inc.: Hoboken, NJ, 2006.
- (63) Munger, J. W.; Wofsy, S. C.; Bakwin, P. S.; Fan, S. M.; Goulden, M. L.; Daube, B. C.; Goldstein, A. H.; Moore, K. E.; Fitzjarrald, D. R. *J. Geophys. Res.: Atmos.* **1996**, *101*, 12639.
- (64) Hill, K. A.; Shepson, P. B.; Galbavy, E. S.; Anastasio, C. *J. Geophys. Res.: Biogeosci.* **2005**, DOI: 10.1029/2005JG000030.
- (65) Farmer, D. K.; Cohen, R. C. *Atmos. Chem. Phys.* **2008**, *8*, 3899.
- (66) Lim, Y. B.; Ziemann, P. J. *Environ. Sci. Technol.* **2005**, *39*, 9229.

- (67) Matsunaga, A.; Docherty, K. S.; Lim, Y. B.; Ziemann, P. J. *Atmos. Environ.* **2009**, *43*, 1349.
- (68) Taylor, W. D.; Allston, T. D.; Moscato, M. J.; Fazekas, G. B.; Kozlowski, R.; Takacs, G. A. *Int. J. Chem. Kinet.* **1980**, *12*, 231.
- (69) Clemitschaw, K. C.; Williams, J.; Rattigan, O. V.; Shallcross, D. E.; Law, K. S.; Cox, R. A. *J. Photochem. Photobiol. A* **1997**, *102*, 117.
- (70) Barnes, I.; Becker, K. H.; Zhu, T. *J. Atmos. Chem.* **1993**, *17*, 353.
- (71) Carbajo, P. G.; Orr-Ewing, A. J. *J. Phys. Chem. Chem. Phys.* **2010**, *12*, 6084.
- (72) Luke, W. T.; Dickerson, R. R.; Nunnermacker, L. J. *J. Geophys. Res.: Atmos.* **1989**, *94*, 14905.
- (73) Roberts, J. M.; Fajer, R. W. *Environ. Sci. Technol.* **1989**, *23*, 945.
- (74) Turberg, M. P.; Giolando, D. M.; Tilt, C.; Soper, T.; Mason, S.; Davies, M.; Klingensmith, P.; Takacs, G. A. *J. Photochem. Photobiol. A* **1990**, *51*, 281.
- (75) Zhu, L.; Kellis, D. *Chem. Phys. Lett.* **1997**, *278*, 41.
- (76) Suarez-Bertoa, R.; Saliu, F.; Bruschi, M.; Rindone, B. *Tetrahedron* **2012**, *68*, 8267.
- (77) O'Brien, J. M.; Shepson, P. B.; Muthuramu, K.; Hao, C.; Niki, H.; Hastie, D. R.; Taylor, R.; Roussel, P. B. *J. Geophys. Res.: Atmos.* **1995**, *100*, 22795.
- (78) Treves, K.; Rudich, Y. *J. Phys. Chem. A* **2003**, *107*, 7809.
- (79) Fischer, R. G.; Kastler, J.; Ballschmiter, K. *J. Geophys. Res.: Atmos.* **2000**, *105*, 14473.
- (80) Schneider, M.; Luxenhofer, O.; Deissler, A.; Ballschmiter, K. *Environ. Sci. Technol.* **1998**, *32*, 3055.
- (81) Atlas, E. *Nature* **1988**, *331*, 426.
- (82) Rosen, R. S.; Wood, E. C.; Wooldridge, P. J.; Thornton, J. A.; Day, D. A.; Kuster, W.; Williams, E. J.; Jobson, B. T.; Cohen, R. C. *J. Geophys. Res.: Atmos.* **2004**, DOI: 10.1029/2003JD004227.
- (83) Day, D. A.; Dillon, M. B.; Wooldridge, P. J.; Thornton, J. A.; Rosen, R. S.; Wood, E. C.; Cohen, R. C. *J. Geophys. Res.: Atmos.* **2003**, DOI: 10.1029/2003JD003685.
- (84) Cleary, P. A.; Wooldridge, P. J.; Millet, D. B.; McKay, M.; Goldstein, A. H.; Cohen, R. C. *Atmos. Chem. Phys.* **2007**, *7*, 1947.
- (85) Cleary, P. A.; Murphy, J. G.; Wooldridge, P. J.; Day, D. A.; Millet, D. B.; McKay, M.; Goldstein, A. H.; Cohen, R. C. *Atmos. Chem. Phys.* **2005**, *5*, 4801.
- (86) Perring, A. E.; Bertram, T. H.; Wooldridge, P. J.; Fried, A.; Heikes, B. G.; Dibb, J.; Crounse, J. D.; Wennberg, P. O.; Blake, N. J.; Blake, D. R.; Singh, H. B.; Cohen, R. C. *Atmos. Chem. Phys.* **2009**, *9*, 1451.
- (87) Parrish, D. D.; Buhr, M. P.; Trainer, M.; Norton, R. B.; Shimshock, J. P.; Fehsenfeld, F. C.; Anlauf, K. G.; Bottenheim, J. W.; Tang, Y. Z.; Wiebe, H. A.; Roberts, J. M.; Tanner, R. L.; Newman, L.; Bowersox, V. C.; Olszyna, K. J.; Bailey, E. M.; Rodgers, M. O.; Wang, T.; Berresheim, H.; Roychowdhury, U. K.; Demerjian, K. L. *J. Geophys. Res.: Atmos.* **1993**, *98*, 2927.
- (88) Nielsen, T.; Egeland, A. H.; Granby, K.; Skov, H. *Atmos. Environ.* **1995**, *29*, 1757.
- (89) Dunlea, E. J.; Herndon, S. C.; Nelson, D. D.; Volkamer, R. M.; San Martini, F.; Sheehy, P. M.; Zahniser, M. S.; Shorter, J. H.; Wormhoudt, J. C.; Lamb, B. K.; Allwine, E. J.; Gaffney, J. S.; Marley, N. A.; Grutter, M.; Marquez, C.; Blanco, S.; Cardenas, B.; Retama, A.; Villegas, C. R. R.; Kolb, C. E.; Molina, L. T.; Molina, M. J. *Atmos. Chem. Phys.* **2007**, *7*, 2691.
- (90) Trainer, M.; Buhr, M. P.; Curran, C. M.; Fehsenfeld, F. C.; Hsie, E. Y.; Liu, S. C.; Norton, R. B.; Parrish, D. D.; Williams, E. J.; Gandrud, B. W.; Ridley, B. A.; Shetter, J. D.; Allwine, E. J.; Westberg, H. H. *J. Geophys. Res.: Atmos.* **1991**, *96*, 3045.
- (91) Fahey, D. W.; Hubler, G.; Parrish, D. D.; Williams, E. J.; Norton, R. B.; Ridley, B. A.; Singh, H. B.; Liu, S. C.; Fehsenfeld, F. C. *J. Geophys. Res.: Atmos.* **1986**, *91*, 9781.
- (92) Buhr, M. P.; Parrish, D. D.; Norton, R. B.; Fehsenfeld, F. C.; Sievers, R. E.; Roberts, J. M. *J. Geophys. Res.: Atmos.* **1990**, *95*, 9809.
- (93) Atherton, C. S.; Penner, J. E. *J. Geophys. Res.: Atmos.* **1990**, *95*, 14027.
- (94) Calvert, J. G.; Madronich, S. *J. Geophys. Res.: Atmos.* **1987**, *92*, 2211.
- (95) Shepson, P. B.; Anlauf, K. G.; Bottenheim, J. W.; Wiebe, H. A.; Gao, N.; Muthuramu, K.; Mackay, G. I. *Atmos. Environ., Part A* **1993**, *27*, 749.
- (96) Flocke, F.; Volzthomas, A.; Kley, D. *Atmos. Environ., Part A* **1991**, *25*, 1951.
- (97) Luxenhofer, O.; Schneider, M.; Dambach, M.; Ballschmiter, K. *Chemosphere* **1996**, *33*, 393.
- (98) Luxenhofer, O.; Ballschmiter, K. *Fresenius' J. Anal. Chem.* **1994**, *350*, 395.
- (99) Luxenhofer, O.; Schneider, E.; Ballschmiter, K. *Fresenius' J. Anal. Chem.* **1994**, *350*, 384.
- (100) Atlas, E.; Schaufler, S. M.; Merrill, J. T.; Hahn, C. J.; Ridley, B.; Walega, J.; Greenberg, J.; Heidt, L.; Zimmerman, P. *J. Geophys. Res.: Atmos.* **1992**, *97*, 10331.
- (101) Atherton, C. S. *Geophys. Res. Lett.* **1989**, *16*, 1289.
- (102) Roberts, J. M.; Parrish, D. D.; Norton, R. B.; Bertman, S. B.; Holloway, J. S.; Trainer, M.; Fehsenfeld, F. C.; Carroll, M. A.; Alberco, G. M.; Wang, T.; Forbes, G. *J. Geophys. Res.: Atmos.* **1996**, *101*, 28947.
- (103) Beine, H. J.; Jaffe, D. A.; Blake, D. R.; Atlas, E.; Harris, J. *J. Geophys. Res.: Atmos.* **1996**, *101*, 12613.
- (104) Bertman, S. B.; Roberts, J. M.; Parrish, D. D.; Buhr, M. P.; Goldan, P. D.; Kuster, W. C.; Fehsenfeld, F. C.; Montzka, S. A.; Westberg, H. *J. Geophys. Res.: Atmos.* **1995**, *100*, 22805.
- (105) Kastler, J.; Ballschmiter, K. *Fresenius' J. Anal. Chem.* **1998**, *360*, 812.
- (106) Kastler, J.; Ballschmiter, K. *Fresenius' J. Anal. Chem.* **1999**, *363*, 1.
- (107) Kastler, J.; Dubourg, V.; Deisenhofer, R.; Ballschmiter, K. *Chromatographia* **1998**, *47*, 157.
- (108) Kastler, J.; Jarman, W.; Ballschmiter, K. *Fresenius' J. Anal. Chem.* **2000**, *368* (2/3), 244.
- (109) Werner, G.; Kastler, J.; Looser, R.; Ballschmiter, K. *Angew. Chem., Int. Ed.* **1999**, *38*, 1634.
- (110) Grossenbacher, J. W.; Couch, T.; Shepson, P. B.; Thornberry, T.; Witmer-Rich, M.; Carroll, M. A.; Faloona, I.; Tan, D.; Brune, W.; Ostling, K.; Bertman, S. *J. Geophys. Res.: Atmos.* **2001**, *106*, 24429.
- (111) Thornberry, T.; Carroll, M. A.; Keeler, G. J.; Sillman, S.; Bertman, S. B.; Pippin, M. R.; Ostling, K.; Grossenbacher, J. W.; Shepson, P. B.; Cooper, O. R.; Moody, J. L.; Stockwell, W. R. *J. Geophys. Res.: Atmos.* **2001**, *106*, 24359.
- (112) Grossenbacher, J. W.; Barket, D. J.; Shepson, P. B.; Carroll, M. A.; Olszyna, K.; Apel, E. *J. Geophys. Res.: Atmos.* **2004**, DOI: 10.1029/2003JD003966.
- (113) Kwok, E. S. C.; Aschmann, S. M.; Arey, J.; Atkinson, R. *Int. J. Chem. Kinet.* **1996**, *28*, 925.
- (114) Bouvier-Brown, N. C.; Goldstein, A. H.; Worton, D. R.; Matross, D. M.; Gilman, J. B.; Kuster, W. C.; Welsh-Bon, D.; Warneke, C.; de Gouw, J. A.; Cahill, T. M.; Holzinger, R. *Atmos. Chem. Phys.* **2009**, *9*, 2061.
- (115) Thornton, J. A.; Wooldridge, P. J.; Cohen, R. C. *Anal. Chem.* **2000**, *72*, 528.
- (116) Paul, D.; Furgeson, A.; Osthoff, H. D. *Rev. Sci. Instrum.* **2009**, *80*, 111101.
- (117) Murphy, J. G.; Day, A.; Cleary, P. A.; Wooldridge, P. J.; Cohen, R. C. *Atmos. Chem. Phys.* **2006**, *6*, 5321.
- (118) Thaler, R. D.; Mielke, L. H.; Osthoff, H. D. *Anal. Chem.* **2011**, *83*, 2761.
- (119) Roberts, J. M.; Osthoff, H. D.; Brown, S. S.; Ravishankara, A. R.; Coffman, D.; Quinn, P.; Bates, T. *Geophys. Res. Lett.* **2009**, *36*, L20808.
- (120) Ghosh, B.; Papanastasiou, D. K.; Talukdar, R. K.; Roberts, J. M.; Burkholder, J. B. *J. Phys. Chem. A* **2012**, *116*, 5796.
- (121) Phillips, G. J.; Tang, M. J.; Thieser, J.; Brickwedde, B.; Schuster, G.; Bohn, B.; Lelieveld, J.; Crowley, J. N. *Geophys. Res. Lett.* **2012**, *39*, L10811.
- (122) Mielke, L. H.; Furgeson, A.; Osthoff, H. D. *Environ. Sci. Technol.* **2011**, *45*, 8889.

- (123) Osthoff, H. D.; Roberts, J. M.; Ravishankara, A. R.; Williams, E. J.; Lerner, B. M.; Sommariva, R.; Bates, T. S.; Coffman, D.; Quinn, P. K.; Dibb, J. E.; Stark, H.; Burkholder, J. B.; Talukdar, R. K.; Meagher, J.; Fehsenfeld, F. C.; Brown, S. S. *Nat. Geosci.* **2008**, *1*, 324.
- (124) Ciccioli, P.; Cecinato, A.; Brancaleoni, E.; Frattoni, M.; Zaccari, P.; Decastrovacconcellos, P. *Ann. Chim.* **1995**, *85*, 455.
- (125) Arey, J.; Zielinska, B.; Atkinson, R. *Abstr. Pap. Am. Chem. Soc.* **1989**, *198*, 16.
- (126) Arey, J.; Zielinska, B.; Atkinson, R.; Winer, A. M.; Ramdahl, T.; Pitts, J. N. *Abstr. Pap. Am. Chem. Soc.* **1986**, *192*, 37.
- (127) Reisen, F.; Arey, J. *Environ. Sci. Technol.* **2005**, *39*, 64.
- (128) Dimashki, M.; Harrad, S.; Harrison, R. M. *Atmos. Environ.* **2000**, *34*, 2459.
- (129) Karavalakis, G.; Boutsika, V.; Stournas, S.; Bakeas, E. *Sci. Total Environ.* **2011**, *409*, 738.
- (130) Nielsen, T.; Seitz, B.; Ramdahl, T. *Atmos. Environ.* **1984**, *18*, 2159.
- (131) Bertram, T. H.; Cohen, R. C.; Thorn, W. J.; Chu, P. M. *J. Air Waste Manage. Assoc.* **2005**, *55*, 1473.
- (132) Wooldridge, P. J.; Perring, A. E.; Bertram, T. H.; Flocke, F. M.; Roberts, J. M.; Singh, H. B.; Huey, L. G.; Thornton, J. A.; Wolfe, G. M.; Murphy, J. G.; Fry, J. L.; Rollins, A. W.; LaFranchi, B. W.; Cohen, R. C. *Atmos. Meas. Tech.* **2010**, *3*, 593.
- (133) Farmer, D. K.; Wooldridge, P. J.; Cohen, R. C. *Atmos. Chem. Phys.* **2006**, *6*, 3471.
- (134) Thornton, J. A.; Wooldridge, P. J.; Cohen, R. C.; Williams, E. J.; Hereid, D.; Fehsenfeld, F. C.; Stutz, J.; Aliche, B. *J. Geophys. Res.: Atmos.* **2003**, DOI: 10.1029/2003JD003559.
- (135) Farmer, D. K.; Perring, A. E.; Wooldridge, P. J.; Blake, D. R.; Baker, A.; Meinardi, S.; Huey, L. G.; Tanner, D.; Vargas, O.; Cohen, R. C. *Atmos. Chem. Phys.* **2011**, *11*, 4085.
- (136) Perring, A. E.; Bertram, T. H.; Farmer, D. K.; Wooldridge, P. J.; Dibb, J.; Blake, N. J.; Blake, D. R.; Singh, H. B.; Fuelberg, H.; Diskin, G.; Sachse, G.; Cohen, R. C. *Atmos. Chem. Phys.* **2010**, *10*, 7215.
- (137) Wu, S. L.; Mickley, L. J.; Jacob, D. J.; Logan, J. A.; Yantosca, R. M.; Rind, D. *J. Geophys. Res.: Atmos.* **2007**, DOI: 10.1029/2006JD007801.
- (138) Ito, A.; Sillman, S.; Penner, J. E. *J. Geophys. Res.: Atmos.* **2007**, DOI: 10.1029/2007JD008745.
- (139) Aschmann, S. M.; Arey, J.; Atkinson, R. *Environ. Sci. Technol.* **2012**, *46*, 13278.
- (140) Atkinson, R.; Arey, J. *Chem. Rev.* **2003**, *103*, 4605.
- (141) Neuman, J. A.; Aikin, K. C.; Atlas, E. L.; Blake, D. R.; Holloway, J. S.; Meinardi, S.; Nowak, J. B.; Parrish, D. D.; Peischl, J.; Perring, A. E.; Pollack, I. B.; Roberts, J. M.; Ryerson, T. B.; Trainer, M. *J. Geophys. Res.: Atmos.* **2012**, DOI: 10.1029/2011jd017150.
- (142) Bloss, C.; Wagner, V.; Jenkin, M. E.; Volkamer, R.; Bloss, W. J.; Lee, J. D.; Heard, D. E.; Wirtz, K.; Martin-Reviejo, M.; Rea, G.; Wenger, J. C.; Pilling, M. J. *Atmos. Chem. Phys.* **2005**, *5*, 641.
- (143) Robinson, A. L.; Donahue, N. M.; Shrivastava, M. K.; Weitkamp, E. A.; Sage, A. M.; Grieshop, A. P.; Lane, T. E.; Pierce, J. R.; Pandis, S. N. *Science* **2007**, *315*, 1259.
- (144) Mao, J.; Ren, X.; Brune, W. H.; Olson, J. R.; Crawford, J. H.; Fried, A.; Huey, L. G.; Cohen, R. C.; Heikes, B.; Singh, H. B.; Blake, D. R.; Sachse, G. W.; Diskin, G. S.; Hall, S. R.; Shetter, R. E. *Atmos. Chem. Phys.* **2009**, *9*, 163.
- (145) Noelscher, A. C.; Williams, J.; Sinha, V.; Custer, T.; Song, W.; Johnson, A. M.; Axinte, R.; Bozem, H.; Fischer, H.; Pouvesle, N.; Phillips, G.; Crowley, J. N.; Rantala, P.; Rinne, J.; Kulmala, M.; Gonzales, D.; Valverde-Canossa, J.; Vogel, A.; Hoffmann, T.; Ouwersloot, H. G.; de Arellano, J. V.-G.; Lelieveld, J. *Atmos. Chem. Phys.* **2012**, *12*, 8257.
- (146) Lou, S.; Holland, F.; Rohrer, F.; Lu, K.; Bohn, B.; Brauers, T.; Chang, C. C.; Fuchs, H.; Haeseler, R.; Kita, K.; Kondo, Y.; Li, X.; Shao, M.; Zeng, L.; Wahner, A.; Zhang, Y.; Wang, W.; Hofzumahaus, A. *Atmos. Chem. Phys.* **2010**, *10*, 11243.
- (147) Ingham, T.; Goddard, A.; Whalley, L. K.; Furneaux, K. L.; Edwards, P. M.; Seal, C. P.; Self, D. E.; Johnson, G. P.; Read, K. A.; Lee, J. D.; Heard, D. E. *Atmos. Meas. Tech.* **2009**, *2*, 465.
- (148) Di Carlo, P.; Brune, W. H.; Martinez, M.; Harder, H.; Lesher, R.; Ren, X. R.; Thornberry, T.; Carroll, M. A.; Young, V.; Shepson, P. B.; Riemer, D.; Apel, E.; Campbell, C. *Science* **2004**, *304*, 722.
- (149) Sinha, V.; Williams, J.; Crowley, J. N.; Lelieveld, J. *Atmos. Chem. Phys.* **2008**, *8*, 2213.
- (150) Sinha, V.; Williams, J.; Lelieveld, J.; Ruuskanen, T. M.; Kajos, M. K.; Patokoski, J.; Hellen, H.; Hakola, H.; Mogensen, D.; Boy, M.; Rinne, J.; Kulmala, M. *Environ. Sci. Technol.* **2010**, *44*, 6614.
- (151) Kovacs, T. A.; Brune, W. H.; Harder, H.; Martinez, M.; Simpas, J. B.; Frost, G. J.; Williams, E.; Jobson, T.; Stroud, C.; Young, V.; Fried, A.; Wert, B. *J. Environ. Monit.* **2003**, *5*, 68.
- (152) Ito, A.; Sillman, S.; Penner, J. E. *J. Geophys. Res.: Atmos.* **2009**, *114*, D09301.
- (153) Browne, E. C.; Cohen, R. C. *Atmos. Chem. Phys.* **2012**, *12*, 11917.
- (154) Taraborrelli, D.; Lawrence, M. G.; Butler, T. M.; Sander, R.; Lelieveld, J. *Atmos. Chem. Phys.* **2009**, *9*, 2751.
- (155) Paulot, F.; Henze, D. K.; Wennberg, P. O. *Atmos. Chem. Phys.* **2012**, *12*, 1307.
- (156) Jacob, D. J.; Winner, D. A. *Atmos. Environ.* **2009**, *43*, 51.
- (157) Xie, Y.; Paulot, F.; Carter, W. P. L.; Nolte, C. G.; Lueken, D. J.; Hutzell, W. T.; Wennberg, P. O.; Cohen, R. C.; Pinder, R. W. *Atmos. Chem. Phys.* **2012**, *12*, 27173.
- (158) Archibald, A. T.; Jenkin, M. E.; Shallcross, D. E. *Atmos. Environ.* **2010**, *44*, 5356.
- (159) Stavrakou, T.; Peeters, J.; Muller, J. F. *Atmos. Chem. Phys.* **2010**, *10*, 9863.
- (160) Carter, W. P. L. *Atmos. Environ.* **2010**, *44*, 5324.
- (161) Fiore, A. M.; Dentener, F. J.; Wild, O.; Cuvelier, C.; Schultz, M. G.; Hess, P.; Textor, C.; Schulz, M.; Doherty, R. M.; Horowitz, L. W.; MacKenzie, I. A.; Sanderson, M. G.; Shindell, D. T.; Stevenson, D. S.; Szopa, S.; Van Dingenen, R.; Zeng, G.; Atherton, C.; Bergmann, D.; Bey, I.; Carmichael, G.; Collins, W. J.; Duncan, B. N.; Faluvegi, G.; Folberth, G.; Gauss, M.; Gong, S.; Hauglustaine, D.; Holloway, T.; Isaksen, I. S. A.; Jacob, D. J.; Jonson, J. E.; Kaminski, J. W.; Keating, T. J.; Lupu, A.; Marmer, E.; Montanaro, V.; Park, R. J.; Pitari, G.; Pringle, K. J.; Pyle, J. A.; Schroeder, S.; Vivanco, M. G.; Wind, P.; Wojcik, G.; Wu, S.; Zuber, A. *J. Geophys. Res.: Atmos.* **2009**, DOI: 10.1029/2008jd010816.
- (162) Xie, Y.; Elleman, R.; Jobson, T.; Lamb, B. *J. Geophys. Res.: Atmos.* **2011**, DOI: 10.1029/2011jd015801.
- (163) Browne, E. C.; Min, K. E.; Wooldridge, P. J.; Apel, E.; Blake, D. R.; Brune, W. H.; Cantrell, C. A.; Cubison, M. J.; Diskin, G. S.; Jimenez, J. L.; Weinheimer, A. J.; Wennberg, P. O.; Wisthaler, A.; Cohen, R. C. *Atmos. Chem. Phys.* **2013**, *13*, 201.
- (164) Muthuramu, K.; Shepson, P. B.; Bottenheim, J. W.; Jobson, B. T.; Niki, H.; Anlauf, K. G. *J. Geophys. Res.: Atmos.* **1994**, *99*, 25369.
- (165) Blake, N. J.; Blake, D. R.; Sive, B. C.; Katzenstein, A. S.; Meinardi, S.; Wingenter, O. W.; Atlas, E. L.; Flocke, F.; Ridley, B. A.; Rowland, F. S. *J. Geophys. Res.: Atmos.* **2003**, DOI: 10.1029/2001jd001467.
- (166) Neu, J. L.; Lawler, M. J.; Prather, M. J.; Saltzman, E. S. *Geophys. Res. Lett.* **2008**, *35*, L13814.
- (167) Dahl, E. E.; Yvon-Lewis, S. A.; Saltzman, E. S. *Geophys. Res. Lett.* **2005**, *32*, L20817.
- (168) Liang, J. Y.; Horowitz, L. W.; Jacob, D. J.; Wang, Y. H.; Fiore, A. M.; Logan, J. A.; Gardner, G. M.; Munger, J. W. *J. Geophys. Res.: Atmos.* **1998**, *103*, 13435.
- (169) Horowitz, L. W.; Liang, J. Y.; Gardner, G. M.; Jacob, D. J. *J. Geophys. Res.: Atmos.* **1998**, *103*, 13451.
- (170) Parrish, D. D.; Ryerson, T. B.; Holloway, J. S.; Neuman, J. A.; Roberts, J. M.; Williams, J.; Stroud, C. A.; Frost, G. J.; Trainer, M.; Hubler, G.; Fehsenfeld, F. C.; Flocke, F.; Weinheimer, A. J. *J. Geophys. Res.: Atmos.* **2004**, DOI: 10.1029/2003jd004226.
- (171) Fiore, A. M.; Horowitz, L. W.; Purves, D. W.; Levy, H.; Evans, M. J.; Wang, Y. X.; Li, Q. B.; Yantosca, R. M. *J. Geophys. Res.: Atmos.* **2005**, DOI: 10.1029/2004jd005485.
- (172) Fiore, A. M.; Levy, H. II; Jaffe, D. A. *Atmos. Chem. Phys.* **2011**, *11*, 1697.

- (173) Stevenson, D. S.; Dentener, F. J.; Schultz, M. G.; Ellingsen, K.; van Noije, T. P. C.; Wild, O.; Zeng, G.; Amann, M.; Atherton, C. S.; Bell, N.; Bergmann, D. J.; Bey, I.; Butler, T.; Cofala, J.; Collins, W. J.; Derwent, R. G.; Doherty, R. M.; Drevet, J.; Eskes, H. J.; Fiore, A. M.; Gauss, M.; Hauglustaine, D. A.; Horowitz, L. W.; Isaksen, I. S. A.; Krol, M. C.; Lamarque, J. F.; Lawrence, M. G.; Montanaro, V.; Muller, J. F.; Pitari, G.; Prather, M. J.; Pyle, J. A.; Rast, S.; Rodriguez, J. M.; Sanderson, M. G.; Savage, N. H.; Shindell, D. T.; Strahan, S. E.; Sudo, K.; Szopa, S. *J. Geophys. Res.: Atmos.* **2006**, DOI: 10.1029/2005jd006338.
- (174) von Kuhlmann, R.; Lawrence, M. G.; Poschl, U.; Crutzen, P. J. *Atmos. Chem. Phys.* **2004**, 4, 1.
- (175) Kroll, J. H.; Seinfeld, J. H. *Atmos. Environ.* **2008**, 42, 3593.
- (176) de Gouw, J. A.; Warneke, C.; Montzka, S. A.; Brioude, J.; Holloway, J. S.; Parrish, D. D.; Fehsenfeld, F. C.; Atlas, E. L.; Weber, R. J.; Flocke, F. M. *Geochim. Cosmochim. Acta* **2009**, 73, A273.
- (177) Jimenez, J. L.; Canagaratna, M. R.; Donahue, N. M.; Prevot, A. S. H.; Zhang, Q.; Kroll, J. H.; DeCarlo, P. F.; Allan, J. D.; Coe, H.; Ng, N. L.; Aiken, A. C.; Docherty, K. S.; Ulbrich, I. M.; Grieshop, A. P.; Robinson, A. L.; Duplissy, J.; Smith, J. D.; Wilson, K. R.; Lanz, V. A.; Hueglin, C.; Sun, Y. L.; Tian, J.; Laaksonen, A.; Raatikainen, T.; Rautiainen, J.; Vaattovaara, P.; Ehn, M.; Kulmala, M.; Tomlinson, J. M.; Collins, D. R.; Cubison, M. J.; Dunlea, E. J.; Huffman, J. A.; Onasch, T. B.; Alfarra, M. R.; Williams, P. I.; Bower, K.; Kondo, Y.; Schneider, J.; Drewnick, F.; Borrmann, S.; Weimer, S.; Demerjian, K.; Salcedo, D.; Cottrell, L.; Griffin, R.; Takami, A.; Miyoshi, T.; Hatakeyama, S.; Shimono, A.; Sun, J. Y.; Zhang, Y. M.; Dzepina, K.; Kimmel, J. R.; Sueper, D.; Jayne, J. T.; Herndorn, S. C.; Trimborn, A. M.; Williams, L. R.; Wood, E. C.; Middlebrook, A. M.; Kolb, C. E.; Baltensperger, U.; Worsnop, D. R. *Science* **2009**, 326, 1525.
- (178) Zhang, Q.; Jimenez, J. L.; Canagaratna, M. R.; Allan, J. D.; Coe, H.; Ulbrich, I.; Alfarra, M. R.; Takami, A.; Middlebrook, A. M.; Sun, Y. L.; Dzepina, K.; Dunlea, E.; Docherty, K.; DeCarlo, P. F.; Salcedo, D.; Onasch, T.; Jayne, J. T.; Miyoshi, T.; Shimono, A.; Hatakeyama, S.; Takegawa, N.; Kondo, Y.; Schneider, J.; Drewnick, F.; Borrmann, S.; Weimer, S.; Demerjian, K.; Williams, P.; Bower, K.; Bahreini, R.; Cottrell, L.; Griffin, R. J.; Rautiainen, J.; Sun, J. Y.; Zhang, Y. M.; Worsnop, D. R. *Geophys. Res. Lett.* **2007**, 34, L13801.
- (179) Volkamer, R.; Jimenez, J. L.; San Martini, F.; Dzepina, K.; Zhang, Q.; Salcedo, D.; Molina, L. T.; Worsnop, D. R.; Molina, M. J. *Geophys. Res. Lett.* **2006**, 33, L17811.
- (180) Dekermenjian, M.; Allen, D. T.; Atkinson, R.; Arey, J. *Aerosol Sci. Technol.* **1999**, 30, 273.
- (181) Gong, H. M.; Matsunaga, A.; Ziemann, P. J. *J. Phys. Chem. A* **2005**, 109, 4312.
- (182) Hallquist, M.; Wangberg, I.; Ljungstrom, E.; Barnes, I.; Becker, K. H. *Environ. Sci. Technol.* **1999**, 33, 553.
- (183) Holes, A.; Eusebi, A.; Grosjean, D.; Allen, D. T. *Aerosol Sci. Technol.* **1997**, 26, 516.
- (184) Palen, E. J.; Allen, D. T.; Pandis, S. N.; Paulson, S. E.; Seinfeld, J. H.; Flagan, R. C. *Atmos. Environ., Part A* **1992**, 26, 1239.
- (185) Presto, A. A.; Hartz, K. E. H.; Donahue, N. M. *Environ. Sci. Technol.* **2005**, 39, 7046.
- (186) Sax, M.; Zenobi, R.; Baltensperger, U.; Kalberer, M. *Aerosol Sci. Technol.* **2005**, 39, 822.
- (187) Surratt, J. D.; Murphy, S. M.; Kroll, J. H.; Ng, A. L. N.; Hildebrandt, L.; Sorooshian, A.; Szmigelski, R.; Vermeylen, R.; Maenhaut, W.; Claeys, M.; Flagan, R. C.; Seinfeld, J. H. *J. Phys. Chem. A* **2006**, 110, 9665.
- (188) Rollins, A. W.; Fry, J. L.; Hunter, J. F.; Kroll, J. H.; Worsnop, D. R.; Singaram, S. W.; Cohen, R. C. *Atmos. Meas. Tech.* **2010**, 3, 301.
- (189) Matsunaga, A.; Ziemann, P. J. *J. Phys. Chem. A* **2009**, 113, 599.
- (190) Hoyle, C. R.; Boy, M.; Donahue, N. M.; Fry, J. L.; Glasius, M.; Guenther, A.; Hallar, A. G.; Hartz, K. H.; Petters, M. D.; Petaja, T.; Rosenoern, T.; Sullivan, A. P. *Atmos. Chem. Phys.* **2011**, 11, 321.
- (191) Kroll, J. H.; Ng, N. L.; Murphy, S. M.; Flagan, R. C.; Seinfeld, J. H. *Geophys. Res. Lett.* **2005**, 32, L18808.
- (192) Kroll, J. H.; Ng, N. L.; Murphy, S. M.; Flagan, R. C.; Seinfeld, J. H. *Environ. Sci. Technol.* **2006**, 40, 1869.
- (193) Ng, N. L.; Chhabra, P. S.; Chan, A. W. H.; Surratt, J. D.; Kroll, J. H.; Kwan, A. J.; McCabe, D. C.; Wennberg, P. O.; Sorooshian, A.; Murphy, S. M.; Dalleska, N. F.; Flagan, R. C.; Seinfeld, J. H. *Atmos. Chem. Phys.* **2007**, 7, 5159.
- (194) Hoyle, C. R.; Berntsen, T.; Myhre, G.; Isaksen, I. S. A. *Atmos. Chem. Phys.* **2007**, 7, 5675.
- (195) Day, D. A.; Liu, S.; Russell, L. M.; Ziemann, P. J. *Atmos. Environ.* **2010**, 44, 1970.
- (196) Garnes, L. A.; Allen, D. T. *Aerosol Sci. Technol.* **2002**, 36, 983.
- (197) Laurent, J. P.; Allen, D. T. *Aerosol Sci. Technol.* **2004**, 38, 82.
- (198) Mylonas, D. T.; Allen, D. T.; Ehrman, S. H.; Pratsinis, S. E. *Atmos. Environ., Part A* **1991**, 25, 2855.
- (199) Russell, L. M.; Bahadur, R.; Ziemann, P. J. *Proc. Natl. Acad. Sci. U.S.A.* **2011**, 108, 3516.
- (200) Mazzoleni, L. R.; Ehrmann, B. M.; Shen, X.; Marshall, A. G.; Collett, J. L., Jr. *Environ. Sci. Technol.* **2010**, 44, 3690.
- (201) Gomez-Gonzalez, Y.; Surratt, J. D.; Cuyckens, F.; Szmigelski, R.; Vermeylen, R.; Jaoui, M.; Lewandowski, M.; Offenberg, J. H.; Kleindienst, T. E.; Edney, E. O.; Blockhuys, F.; Van Alsenoy, C.; Maenhaut, W.; Claeys, M. *J. Mass Spectrom.* **2008**, 43, 371.
- (202) Gomez-Gonzalez, Y.; Wang, W.; Vermeylen, R.; Chi, X.; Neirynck, J.; Janssens, I. A.; Maenhaut, W.; Claeys, M. *Atmos. Chem. Phys.* **2012**, 12, 125.
- (203) Nguyen, T. B.; Laskin, J.; Laskin, A.; Nizkorodov, S. A. *Environ. Sci. Technol.* **2011**, 45, 6908.
- (204) Surratt, J. D.; Gomez-Gonzalez, Y.; Chan, A. W. H.; Vermeylen, R.; Shahgholi, M.; Kleindienst, T. E.; Edney, E. O.; Offenberg, J. H.; Lewandowski, M.; Jaoui, M.; Maenhaut, W.; Claeys, M.; Flagan, R. C.; Seinfeld, J. H. *J. Phys. Chem. A* **2008**, 112, 8345.
- (205) Surratt, J. D.; Kroll, J. H.; Kleindienst, T. E.; Edney, E. O.; Claeys, M.; Sorooshian, A.; Ng, N. L.; Offenberg, J. H.; Lewandowski, M.; Jaoui, M.; Flagan, R. C.; Seinfeld, J. H. *Environ. Sci. Technol.* **2007**, 41, 517.
- (206) Worton, D. R.; Goldstein, A. H.; Farmer, D. K.; Docherty, K. S.; Jimenez, J. L.; Gilman, J. B.; Kuster, W. C.; de Gouw, J.; Williams, B. J.; Kreisberg, N. M.; Hering, S. V.; Bench, G.; McKay, M.; Kristensen, K.; Glasius, M.; Surratt, J. D.; Seinfeld, J. H. *Atmos. Chem. Phys.* **2011**, 11, 10219.
- (207) Bruns, E. A.; Perraud, V.; Zelenyuk, A.; Ezell, M. J.; Johnson, S. N.; Yu, Y.; Imre, D.; Finlayson-Pitts, B. J.; Alexander, M. L. *Environ. Sci. Technol.* **2010**, 44, 1056.
- (208) Farmer, D. K.; Matsunaga, A.; Docherty, K. S.; Surratt, J. D.; Seinfeld, J. H.; Ziemann, P. J.; Jimenez, J. L. *Proc. Natl. Acad. Sci. U.S.A.* **2010**, 107, 6670.
- (209) Rollins, A. W.; Browne, E. C.; Min, K. E.; Pusede, S. E.; Wooldridge, P. J.; Gentner, D. R.; Goldstein, A. H.; Liu, S.; Day, D. A.; Russell, L. M.; Cohen, R. C. *Science* **2012**, 337, 1210.
- (210) Allen, D. T.; Palen, E. J.; Haimov, M. I.; Hering, S. V.; Young, J. R. *Aerosol Sci. Technol.* **1994**, 21, 325.
- (211) Pratt, K. A.; Prather, K. A. *Mass Spectrom. Rev.* **2012**, 31, 17.
- (212) Iinuma, Y.; Muller, C.; Berndt, T.; Boge, O.; Claeys, M.; Herrmann, H. *Environ. Sci. Technol.* **2007**, 41, 6678.
- (213) Altieri, K. E.; Hastings, M. G.; Peters, A. J.; Sigman, D. M. *Atmos. Chem. Phys.* **2012**, 12, 3557.
- (214) Altieri, K. E.; Turpin, B. J.; Seitzinger, S. P. *Atmos. Chem. Phys.* **2009**, 9, 2533.
- (215) Altieri, K. E.; Turpin, B. J.; Seitzinger, S. P. *Environ. Sci. Technol.* **2009**, 43, 6950.
- (216) Allan, J. D.; Delia, A. E.; Coe, H.; Bower, K. N.; Alfarra, M. R.; Jimenez, J. L.; Middlebrook, A. M.; Drewnick, F.; Onasch, T. B.; Canagaratna, M. R.; Jayne, J. T.; Worsnop, D. R. *J. Aerosol Sci.* **2004**, 35, 909.
- (217) Jayne, J. T.; Leard, D. C.; Zhang, X. F.; Davidovits, P.; Smith, K. A.; Kolb, C. E.; Worsnop, D. R. *Aerosol Sci. Technol.* **2000**, 33, 49.
- (218) Jimenez, J. L.; Jayne, J. T.; Shi, Q.; Kolb, C. E.; Worsnop, D. R.; Yourshaw, I.; Seinfeld, J. H.; Flagan, R. C.; Zhang, X. F.; Smith, K. A.; Morris, J. W.; Davidovits, P. *J. Geophys. Res.: Atmos.* **2003**, DOI: 10.1029/2001jd001213.

- (219) Zhang, Q.; Jimenez, J. L.; Worsnop, D. R.; Canagaratna, M. *Environ. Sci. Technol.* **2007**, *41*, 3213.
- (220) Zhang, Q.; Alfarra, M. R.; Worsnop, D. R.; Allan, J. D.; Coe, H.; Canagaratna, M. R.; Jimenez, J. L. *Environ. Sci. Technol.* **2005**, *39*, 4938.
- (221) de Gouw, J. A.; Middlebrook, A. M.; Warneke, C.; Goldan, P. D.; Kuster, W. C.; Roberts, J. M.; Fehsenfeld, F. C.; Worsnop, D. R.; Canagaratna, M. R.; Pszenny, A. A. P.; Keene, W. C.; Marchewka, M.; Bertman, S. B.; Bates, T. S. *J. Geophys. Res.: Atmos.* **2005**, DOI: 10.1029/2004jd005623.
- (222) Johnson, K. S.; de Foy, B.; Zuberi, B.; Molina, L. T.; Molina, M. J.; Xie, Y.; Laskin, A.; Shutthanandan, V. *Atmos. Chem. Phys.* **2006**, *6*, 4591.
- (223) Kondo, Y.; Miyazaki, Y.; Takegawa, N.; Miyakawa, T.; Weber, R. J.; Jimenez, J. L.; Zhang, Q.; Worsnop, D. R. *J. Geophys. Res.: Atmos.* **2007**, DOI: 10.1029/2006jd007056.
- (224) Takegawa, N.; Miyakawa, T.; Kondo, Y.; Blake, D. R.; Kanaya, Y.; Koike, M.; Fukuda, M.; Komazaki, Y.; Miyazaki, Y.; Shimono, A.; Takeuchi, T. *Geophys. Res. Lett.* **2006**, *33*, L15814.
- (225) Bae, M.-S.; Schwab, J. J.; Zhang, Q.; Hogrefe, O.; Demerjian, K. L.; Weimer, S.; Rhoads, K.; Orsini, D.; Venkatachari, P.; Hopke, P. K. *J. Geophys. Res.: Atmos.* **2007**, *112*, D22305.
- (226) Baker, J. W.; Easty, D. M. *Nature* **1950**, *166*, 156.
- (227) Darer, A. I.; Cole-Filipliak, N. C.; O'Connor, A. E.; Elrod, M. J. *Environ. Sci. Technol.* **2011**, *45*, 1895.
- (228) Hu, K. S.; Darer, A. I.; Elrod, M. J. *Atmos. Chem. Phys.* **2011**, *11*, 8307.
- (229) Sato, K. *Atmos. Environ.* **2008**, *42*, 6851.
- (230) Liu, S.; Shilling, J. E.; Song, C.; Hiranuma, N.; Zaveri, R. A.; Russell, L. M. *Aerosol Sci. Technol.* **2012**, *46*, 1359.
- (231) Cole-Filipliak, N. C.; O'Connor, A. E.; Elrod, M. J. *Environ. Sci. Technol.* **2010**, *44*, 6718.
- (232) Eddingsaas, N. C.; VanderVelde, D. G.; Wennberg, P. O. *J. Phys. Chem. A* **2010**, *114*, 8106.
- (233) Minerath, E. C.; Elrod, M. J. *Environ. Sci. Technol.* **2009**, *43*, 1386.
- (234) Lockwood, A. L.; Filley, T. R.; Rhodes, D.; Shepson, P. B. *Geophys. Res. Lett.* **2008**, *35*, L15809.
- (235) Ranschaert, D. L.; Schneider, N. J.; Elrod, M. J. *J. Phys. Chem. A* **2000**, *104*, 5758.
- (236) Lightfoot, P. D.; Cox, R. A.; Crowley, J. N.; Destriau, M.; Hayman, G. D.; Jenkin, M. E.; Moortgat, G. K.; Zabel, F. *Atmos. Environ., Part A* **1992**, *26*, 1805.
- (237) Le Bras, G.; Becker, K. H.; Cox, R. A.; Moortgat, G. K.; Sidebottom, H. W.; Zellner, R.; Barnes, I.; Wayne, R. P. *Chemical Processes in Atmospheric Oxidation: Laboratory studies of chemistry related to tropospheric ozone*; Springer: Berlin-Heidelberg, 1997.
- (238) Atkinson, R.; Aschmann, S. M.; Carter, W. P. L.; Winer, A. M.; Pitts, J. N. *Int. J. Chem. Kinet.* **1984**, *16*, 1085.
- (239) Takagi, H.; Washida, N.; Bandow, H.; Akimoto, H.; Okuda, M. *J. Phys. Chem.* **1981**, *85*, 2701.
- (240) Aschmann, S. M.; Chew, A. A.; Arey, J.; Atkinson, R. *J. Phys. Chem. A* **1997**, *101*, 8042.
- (241) Atkinson, R.; Aschmann, S. M.; Winer, A. M.; Pitts, J. N. *Environ. Sci. Technol.* **1984**, *18*, 370.